Article

Preparation and biophysical characterization of Quercetin inclusion complexes with #-cyclodextrin derivatives for the preparation of possible nose-to-brain Quercetin delivery systems

Konstantina Manta, Paraskevi Papakyriakopoulou, Maria Chountoulesi, Dimitrios Diamantis, Dimitrios Spaneas, Vasiliki Vakali, Nikolaos Naziris, Maria Chatziathanasiadou, Ioannis Andreadelis, Kalliopi Moschovou, Ioanna Athanasiadou, Paraskevas Dallas, Dimitrios Rekkas, Costas Demetzos, Gaia Colombo, Sabrina Banella, Uroš Javornik, Janez Plavec, Thomas Mavromoustakos, Andreas G. Tzakos, and Georgia Valsami

Mol. Pharmaceutics, **Just Accepted Manuscript** • DOI: 10.1021/acs.molpharmaceut.0c00672 • Publication Date (Web): 28 Sep 2020

	of Pharmacy, Pharmacy

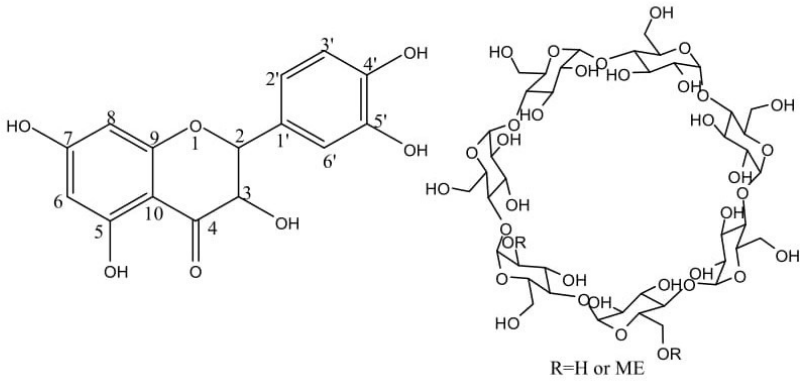

Structures of Que and Me-β-CD

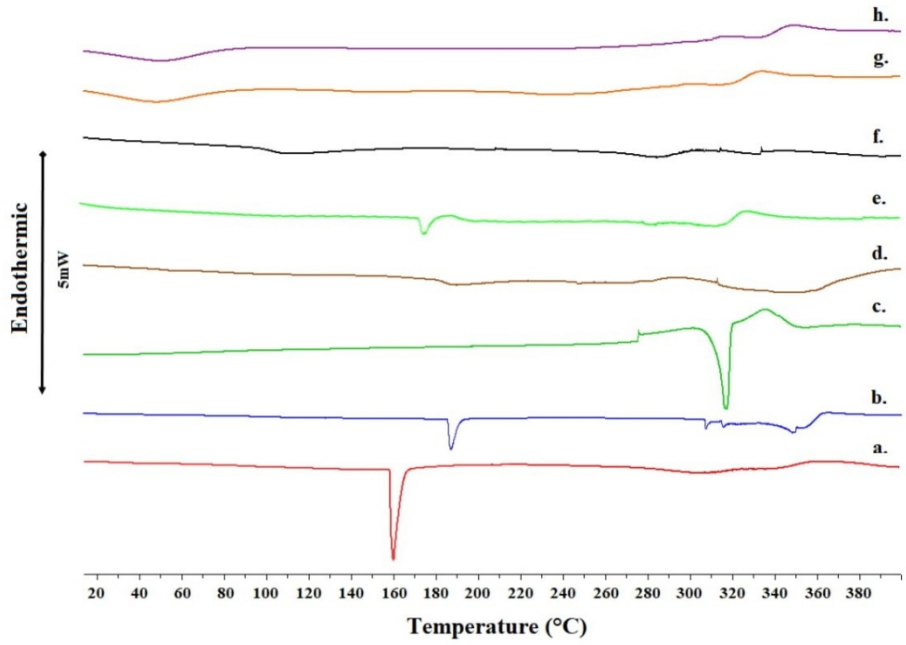

DSC curves of: a) Hydroxypropyl-β-cyclodextrin (HP-β-CD), b). Methyl-β-cyclodextrin (Me-β-CD), c) Quercetin (Que), d) Que:HP-β-CD 1:2 mixture, e) Que:Me-β-CD 1:1 mixture, f) Que:HP-β-CD 1:2 complex, g) Que:Me-β-CD 1:1 complex and h) Que:Me-β-CD 1:2 complex. The double-headed arrow symbol represents a heat flow amount of 5 mW.

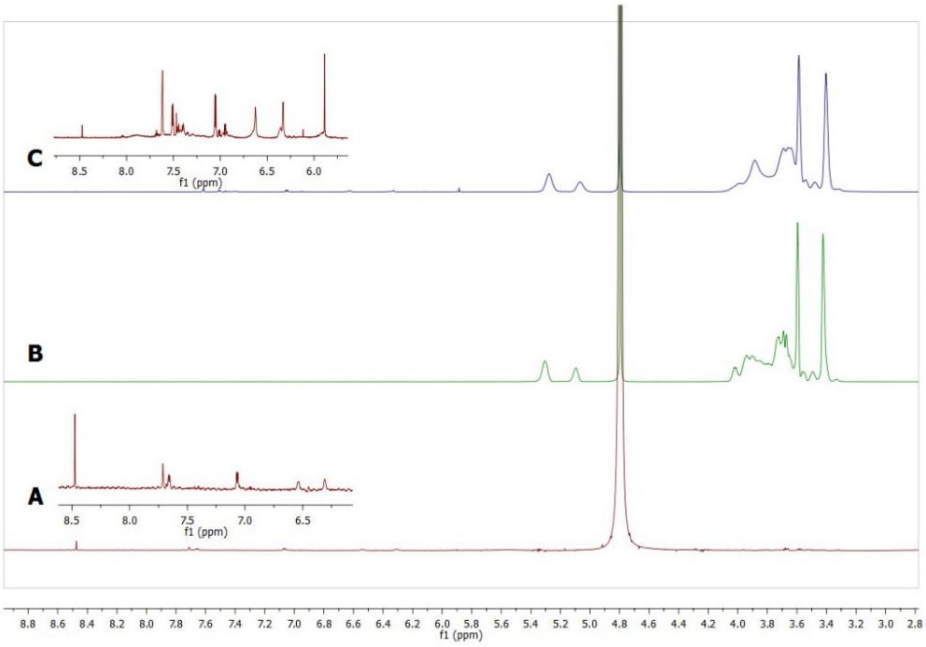

The ^{1}H NMR of (A) complex of Que with Me-β-CD (B) Me-β-CD (C) mixture of QUE with Me-β-CD. The spectra were obtained at 25 °C in D_2O.

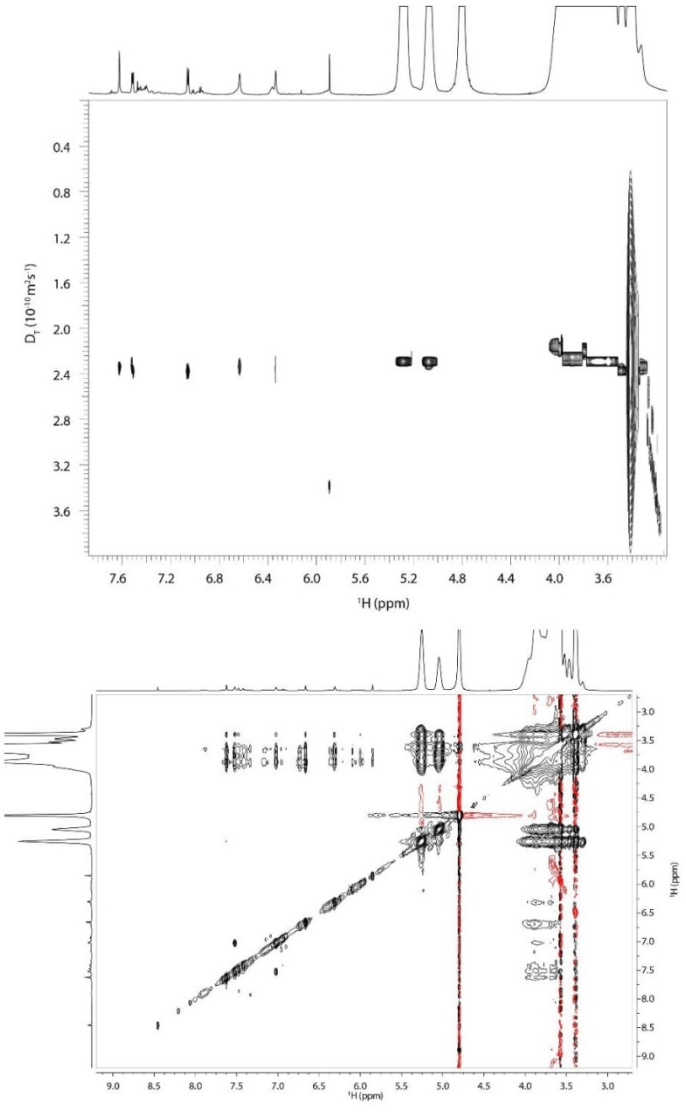

(A): The 2D DOSY experiment of the complex of QUE with Me-β-CD. The spectrum was obtained at 25 °C in D_2O. (B): The 2D NOESY experiment of the complex of QUE with Me-β-CD. The spectrum was obtained at 25 °C in D_2O and using mixing time of 800 ms.

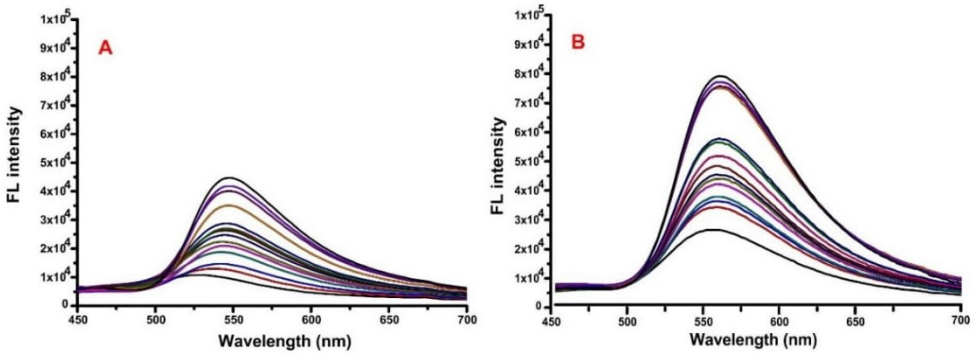

Fluorescence spectra of Que after titrating with various concentrations of HP-β-CD (0, 0.1, 0.2 ,0.3 ,0.4 ,0.5 0.6 ,0.7, 0.8 ,0.9, 1.0 ,2.0 ,3.0 ,4.0 and 5.0 mM) at pH 4.5 (A) and 6.8 (B), respectively.

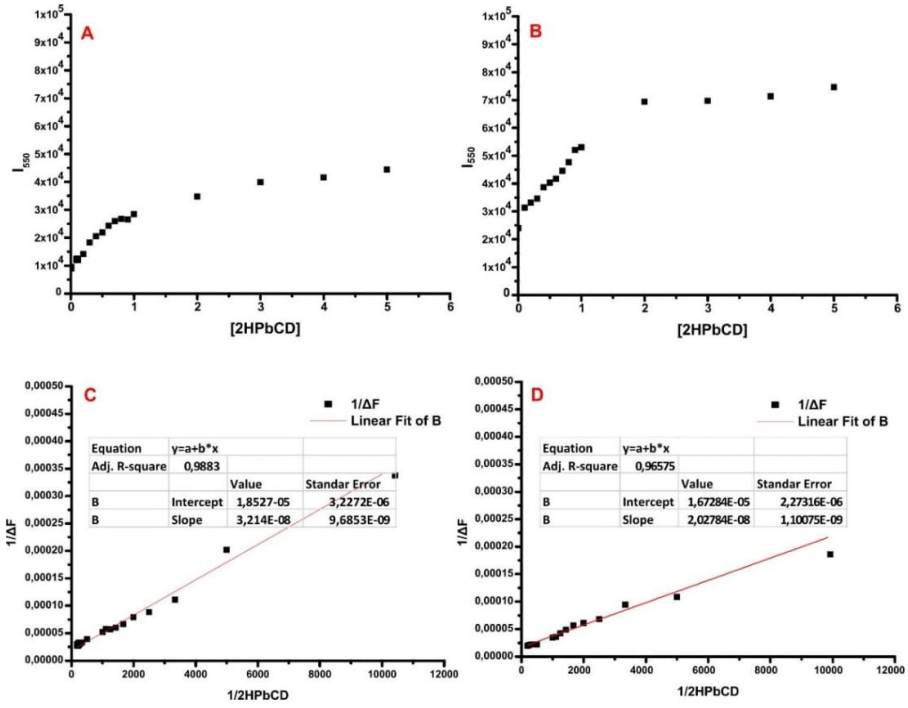

I_{550} of Que after the titration with various HP-β-CD concentrations (0, 0.1, 0.2, 0.3, 0.4, 0.5 0.6, 0.7, 0.8, 0.9, 1.0, 2.0, 3.0, 4.0 and 5.0 mM) at pH 4.5 (A) and 6.8 (B), respectively. C and D represent the double-reciprocal plots as they were derived from the data of A and B, respectively.

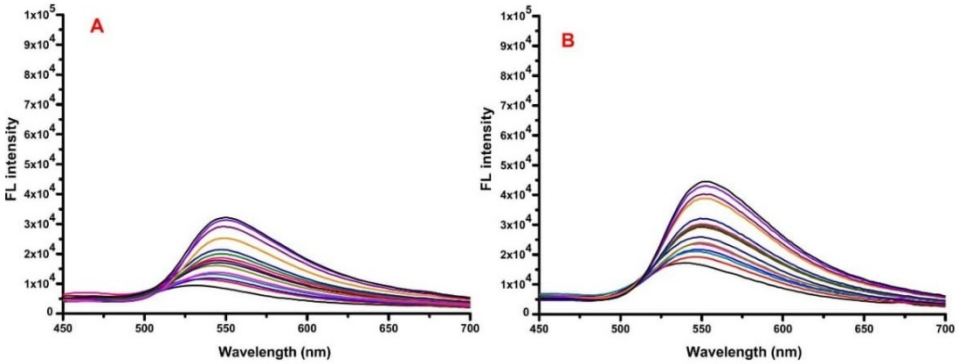

Fluorescence spectra of Que after the titration with various Me-β-CD concentrations (0, 0.1, 0.2 ,0.3 ,0.4 ,0.5 0.6 ,0.7, 0.8 ,0.9, 1.0 ,2.0 ,3.0 ,4.0 and 5.0 mM) at pH 4.5 (A) and 6.8 (B), respectively.

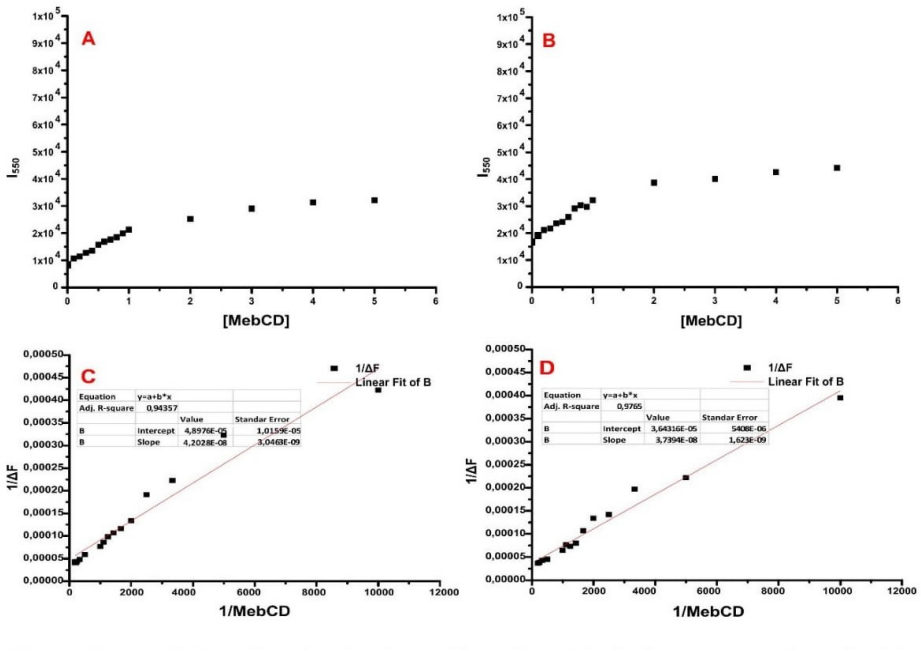

I_{550} of Que after the titration with various Me-β-CD concentrations (0, 0.1, 0.2, 0.3, 0.4, 0.5 0.6, 0.7, 0.8, 0.9, 1.0, 2.0, 3.0, 4.0 and 5.0 mM) at pH 4.5 (A) and 6.8 (B), respectively and D represent the double reciprocal plots as they were derived from the data of A and B, respectively.

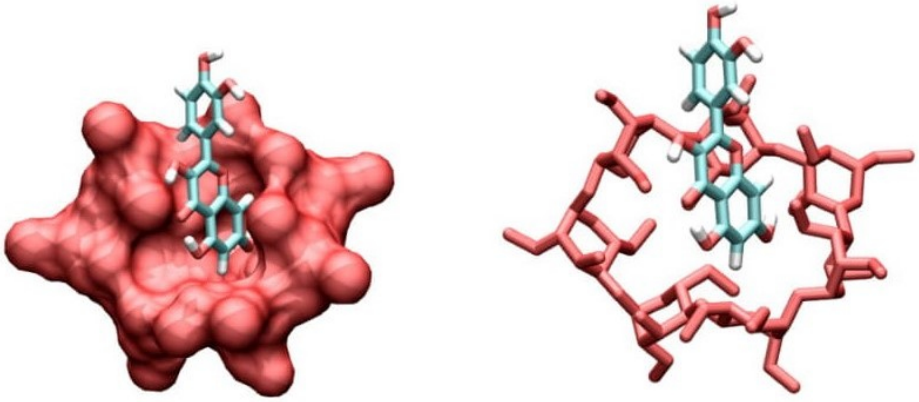

The complex of quercetin and methyl-β-cyclodextrin as it derived from the MD simulations. At the left part of the figure emphasis is given in the cavity where the hydrophobic segment of quercetin is embedded while in the right emphasis is given in the details of the interactions between the two molecules.

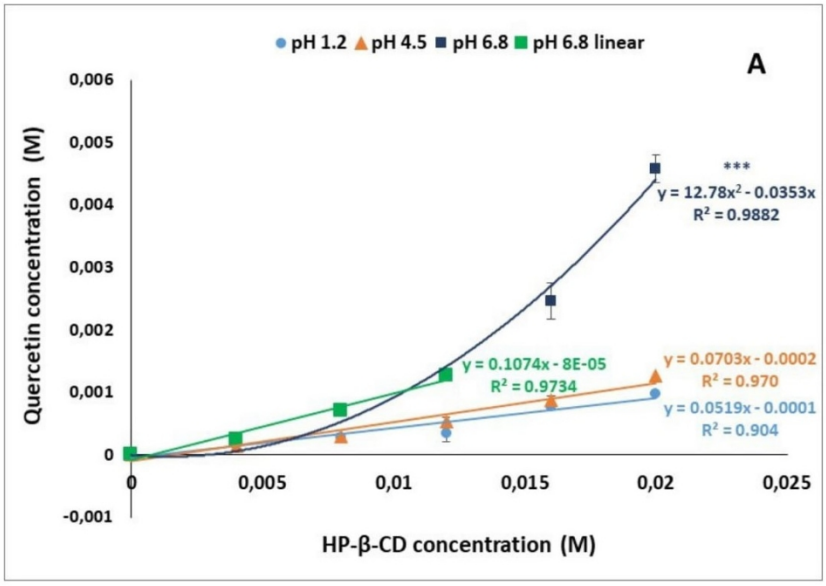

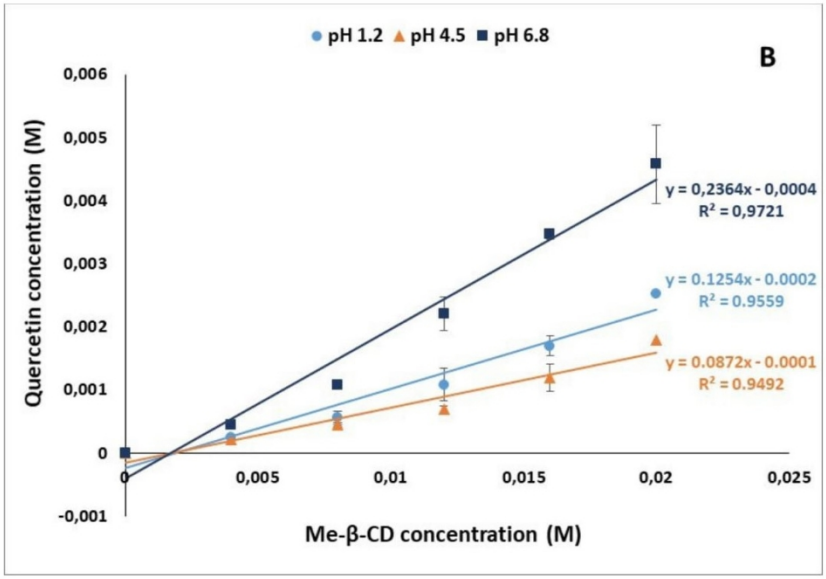

(A) Effect of HP-β-CD and pH on the water solubility of pure Que. (*** Possible formation of a complex involving more than one molecule of cyclodextrin). (B) Effect of Me-β-CD and pH on the water solubility of pure Que. Water solubility of Que was found significant greater at pH 6.8 than in 4.5 and 1.2, respectively ($p<0.05$, paired Student's t-test)

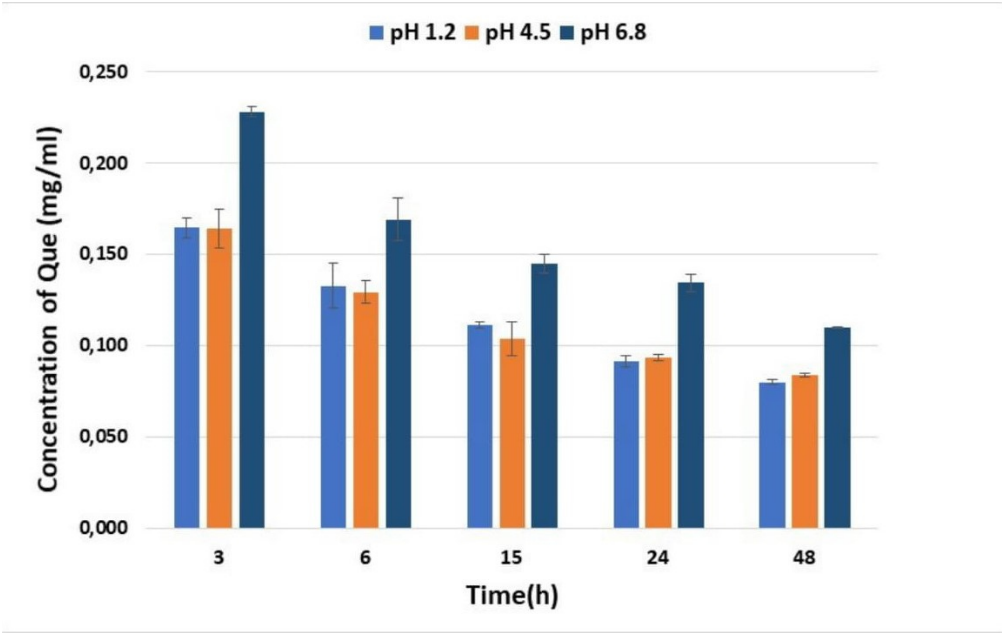

Effect of pH on the solubility of Que-Me-β-CD lyophilized complex. (* Water solubility of Que-Me-β-CD lyophilized complex was found significantly greater at pH 6.8 than in 4.5 and 1.2, at all-time points ($p<0.05$, paired Student's t-test).

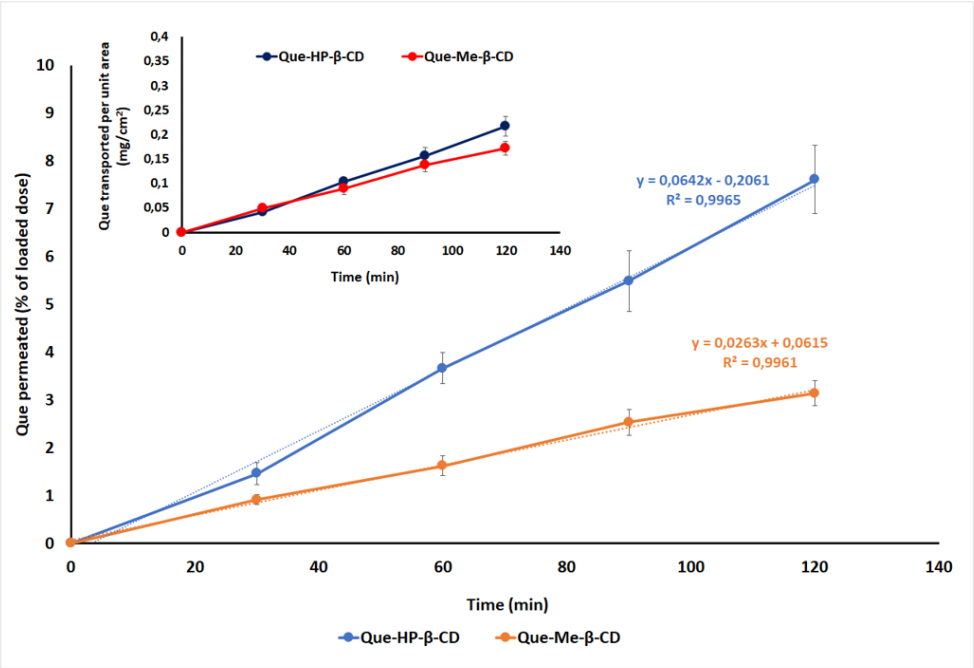

Permeation profiles across rabbit nasal mucosa of Que-HP-β-CD and Que-Me-β-CD lyophilized formulations, expressed as % of the loaded dose (mean ± SEM) vs time, for 2 hours experiments (n=6) and cumulative Que amount permeated per unit area Vs time (Insert graph)

223x154mm (120 x 120 DPI)

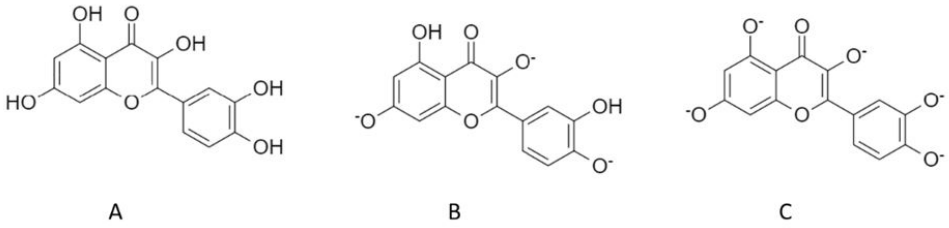

A) Structure of Que, B, C) Deprotonated forms of Que

Preparation and biophysical characterization of Quercetin inclusion complexes with β-cyclodextrin derivatives for the preparation of possible nose-to-brain Quercetin delivery systems

Konstantina Manta [†,#]; Paraskevi Papakyriakopoulou [†,#]; Maria Chountoulesi [†]; Dimitrios A. Diamantis [‡]; Dimitrios Spaneas[†], Vasiliki Vakali [ǁ]; Nikolaos Naziris [†]; Maria V. Chatziathanasiadou [‡]; Ioannis Andreadelis[ǁ], Kalliopi Moschovou[ǁ], Ioanna Athanasiadou [†]; Paraskevas Dallas [†]; Dimitrios M. Rekkas [†]; Costas Demetzos [†]; Gaia Colombo[*]; Sabrina Banella[*]; Uroš Javornik [§]; Janez Plavec [§]; Thomas Mavromoustakos [ǁ]; Andreas G. Tzakos [‡,▪]; Georgia Valsami [†*]

† Department of Pharmacy, School of Health Sciences, National and Kapodistrian University of Athens, Zografou 15771, Greece

ǁ Department of Chemistry, School of Sciences, National and Kapodistrian University of Athens, Panepistimiopolis Zografou 15771, Greece

‡ Department of Chemistry, Section of Organic Chemistry and Biochemistry, University of Ioannina, Ioannina 45110, Greece

▪ University Reasearch Center of Ioannina (URCI), Institute of Materials Science and Computing, Ioannina 45110, Greece

* Department of Life Sciences and Biotechnology, University of Ferrara, Italy,

§ Slovenian NMR Centre, National Institute of Chemistry, Slovenia

# equal contribution

* Correspondence:
Georgia Valsami
Department of Pharmacy, School of Health Sciences, National and Kapodistrian University of Athens, Zografou 15771, Greece
e-mail: valsami@pharm.uoa.gr;
Tel.+302107274022
Fax: +302107274027

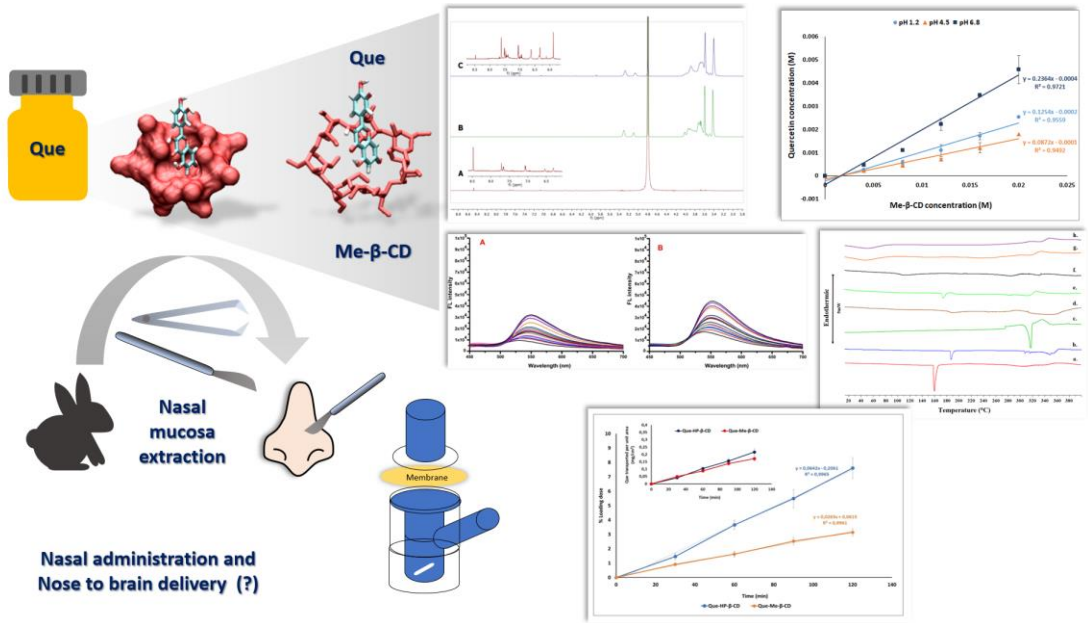

Graphical Abstract

Abstract: Quercetin (Que) is a flavonoid associated with high oxygen radical scavenging activity, and potential neuroprotective activity against Alzheimer's disease. Quercetin's oral bioavailability is limited by its low water-solubility and extended peripheral metabolism; thus, nasal administration may be a promising alternative to achieve effective Que concentrations in the brain. The formation of Quercetin-Hydroxypropyl-β-Cyclodextrin (Que-HP-β-CD) complexes was previously found to increase the molecule's solubility and stability in aqueous media. Quercetin-Methyl-β-Cyclodextrin (Que-Me-β-CD) inclusion complexes were prepared, characterized and compared with the Que-HP-β-CD complex using biophysical and computational methods (phase solubility, fluorescence and NMR Spectroscopy, Differential Scanning Calorimetry-DSC, Molecular Dynamics simulations-MDS), as candidates for preparation of nose-to-brain Quercetin's delivery systems. DSC thermograms, NMR, fluorescence spectroscopy and MDS confirmed the inclusion complex formation of Quercetin with both CDs. Differences between the two preparations were observed regarding their thermodynamic stability and inclusion mode governing the details of molecular interactions. Quercetin's solubility in aqueous media at pH 1.2 and 4.5 was similar and linearly increased with both CD concentrations. At pH 6.8 Que's solubility was higher and positively deviating from linearity in presence of HP-β-CD more than with Me-β-CD, possibly revealing the presence of more than one HP-β-CD molecule involved in the complex. Overall, water-solubility of lyophilized Que-Me-β-CD and Que-HP-β-CD products was approximately 7-40 times and 14-50 times as higher as for pure Quercetin at pH 1.2-6.8. In addition, the proof of concept experiment on *ex-vivo* permeation across rabbit nasal mucosa revealed measurable and similar Que permeability profiles with both CDs and negligible permeation of pure Que. These results are quite encouraging for further *ex vivo* and *in vivo* evaluation toward nasal administration and nose-to brain delivery of Que.

Keywords: quercetin; cyclodextrins inclusion complexes; nasal delivery; nasal permeation; phase solubility; NMR and fluorescence spectroscopy; DSC; Molecular Dynamics simulations

INTRODUCTION

Quercetin (Que, Scheme 1) is a natural product, member of the polyphenolic compounds called "Flavonoids" and is found in various fruits, vegetables and pulses. Que is known for its antioxidant properties attributed to high oxygen radical scavenging activity, ascribed to a catechol group in the B ring, a 2,3 -double bond in conjugation with a 4-oxo function in the C ring and OH groups located at positions 3 and 5 in the heterocyclic ring.[1] These groups are optimally configured to neutralize free radicals. The ability of these groups to scavenge free radicals such as $O_2^{\cdot -}$ and $ONOO^-$, makes it one of the most widespread and effective antioxidants.[2] Such radicals could have harmful effects in cells and body tissues. Furthermore, they are related to the occurrence of cardiovascular and neurogenerative diseases, diabetes and cancer.[3]

Concerning its physicochemical properties, Que has low aqueous solubility, low bioavailability after oral administration and is characterized by chemical instability.[4] It is a lipophilic molecule that exhibits moderate solubility in ethanol (4 mg/mL at 37 ° C) and high solubility in dimethylsulfoxide (150 mg / mL at 25 °C). Moreover, its solubility in water is limited to 0.01 mg/mL at 25 °C.[5] Overall, Que is characterized by poor absorption after oral administration. Specifically, the amount of Que which is eventually absorbed is measured about 20% of the initially administered dose.[6]

Although, Que is widely known and used, as a dietary supplement, its pharmaceutical use is limited significantly by the low bioavailability. Several studies reported the formation of inclusion complexes between Que and Cyclodextrins (CDs), as a strategy to enhance Que' s solubility.[7-9]

CDs are a group of cyclic oligosaccharides consisting of sugar monomers (α-D-glycopyranose), which are linked by α- [1,4] -glycosidic bonds. Glycopyranose units' configuration results in the formation of CD molecules as conical frustum which can host a variety of guest molecules in their cavity. This internal cavity of the CD molecule presents hydrophobic character and enables the trapping of lipophilic guest molecules, whereas the outer surface is hydrophilic enhancing water solubility and oral bioavailability of the entrapped lipophilic molecule.[10] The natural α, β and γ CDs consist of 6, 7 and 8 glucose units, respectively. Apart from these naturally occurring CDs, many derivatives have been synthesized such as randomly methylated derivatives of β-CD (RM-β-CD), 2-hydroxypropylated β- and γ-CDs (HP-β-CD, HP-γ-CD), sulfobutylated-β-CDs (SBE-β-CD), branched CDs (glucosyl- and maltosyl-β-CDs), acetylated β- and γ-CDs and sulfated CDs.[11] These host compounds have been utilized in numerous applications, such as the enhancement of solubility, dissolution rate, stability and bioavailability as well as the modification of the drug release profile, the drug toxicity or unpleasant smell / taste reduction and the prevention of drug-drug interactions.[12]

Increasing interest has recently been raised on determining Que's potential neuroprotective action in the nervous system, especially in Alzheimer's disease.[13] Due to low bioavailability and extended peripheral metabolism, nasal administration could be promising to by-pass blood-brain barrier and achieve effective concentrations in the brain.[14] However, Que itself exhibits low permeability across the nasal mucosa due to its low water solubility that hinders the possibility to have highly concentrated solutions for diffusion. The formation of HP-β-CD complexes with Que, was recently found to substantially increase molecule's solubility and stability[8] and accordingly, may also improve its mucosa permeability. Furthermore, CDs interact with nasal epithelial membranes and transiently open tight junctions,[15] facilitating even further the molecule's permeability through nasal mucosa.

The aim of the present study is to prepare and characterize Que's inclusion complexes with Me-β-CD (Scheme 1) and compare them with those of HP-β-CD using various biophysical methods. In addition, a comparative study is being presented aiming to determine the effect of Me-β-CD and HP-β-CD on Que's aqueous solubility. The effect of CDs in aqueous solubility of Que was tested in three different pH values (1.2, 4.5, 6.8) according to the guidelines of EMA[16] for oral formulations. The greater solubility shown at pH 6.8 in presence of either HP-β-CD or Me-β-CD, lead us to consider the preparation of possible nose-to-brain Que delivery systems. More precisely, nasal pH conditions[2] could permit the solubilization of powders in nasal fluids facilitating the permeation through the mucosa. This hypothesis is also supported by an *ex-vivo* permeability proof of concept study indicating the greater permeability of lyophilized products of Que with the CDs in comparison with the pure Que.

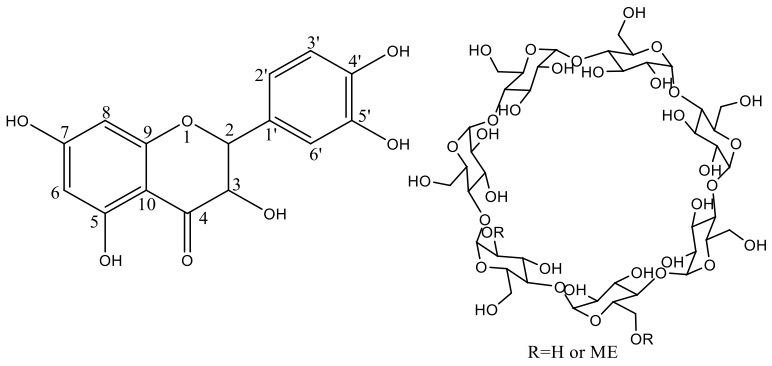

Scheme 1: Structures of Que and Me-β-CD

MATERIALS AND METHODS

Chemicals

Que (MW: 302.24 g/mol), Me-β-CD (MW: 1310 g/mol), HP-β-CD (MW: 1460 g/mol) were purchased from Sigma-Aldrich (St Louis, MO, USA), Fluka Chemika (Mexico City, Mexico US & Canada) and Ashland (Covington, KY, USA), respectively. HPLC grade solvents and reagents were obtained from E. Merck (Darmstadt, Germany) and Fischer Chemical (Pittsburgh, PA, USA). Triple-deionized water from Millipore was used for all preparations.

Complex preparation

Lyophilized formulations of Que-HP-β-CD and Que-Me-β-CD were prepared by freeze-drying aqueous solutions of Que-HP-β-CD and Que-Me-β-CD, using the neutralization method,[17]in molar ratios of 1:2 and 1:1, respectively. More specifically, 2.17 g of Me-β-CD were weighed accurately, transferred into a 600 mL beaker and suspended with 500 mL of water, until the complete CD's solubilization. Under continuous stirring and light protection (due to Que photosensitivity), 500 mg of Que were added to the beaker and formation of suspension was observed. Small amounts of ammonium hydroxide were then added until Que complete dissolution while pH was continuously monitored and adjusted to approximately 9-9.5. The obtained solution was partitioned into round trays for lyophilization, frozen at -73 °C and freeze-dried using Biobase Vacuum Freeze Dryer, BK-FD10T, Biobase biodustry (Shandong) CO., LTD. For the preparation of Que-HP-β-CD 4.8 g of HP-β-CD were weighed and the same procedure was followed as with Me-β-CD.

Differential Scanning Calorimetry (DSC)

The thermodynamic behavior of HP-β-CD, Me-β-CD, Que, their mixtures and lyophilized formulations was studied using, a DSC 822^e Mettler-Toledo calorimeter (Schwerzenbach, Switzerland), after calibration with pure indium (T_m = 156.6 °C). For each analysis, approximately 3 mg of dry powder were weighed inside a 40 μL aluminum crucible, which was then sealed and left for 15 min, in order to achieve equilibration of the sample. Each analysis included a 5 min isotherm at 10 °C and a heating scan from 10 °C to 400 °C, at a heating rate of 5 °C / min, under constant nitrogen gas flow rate of 50 mL / min. The calorimetric data obtained (characteristic transition temperatures T_{onset} and T, enthalpy change ΔH and width at half peak height of the C_p profiles $\Delta T_{1/2}$) were analyzed using Mettler-Toledo STAR^e software (Schwerzenbach, Switzerland). The transition enthalpy was considered positive during an endothermic process.

High resolution ^{1}H NMR spectroscopy

Spectra of Que complexes were recorded on an Agilent Technologies DD2 600 MHz NMR spectrometer with a 5 mm HCN cold probe. ^{1}H NMR spectra were recorded with 65536 points, 90° pulse, 10 s relaxation delay and 32 repetitions. NOESY spectra were recorded at different mixing times with 4096x200 points, 1 s relaxation delay and 32 repetitions per spectrum. The DgcsteSL_cc sequence was used to record DOSY spectra with 65536 points, 1 s relaxation delay and 16 repetitions. 24 gradient strengths between zero and 60 gauss/cm were used. All spectra were recorded at 25 °C. Chemical shifts are referenced with respect to the lock frequency and reported relative to TMS.

Fluorescence Spectroscopic Studies

Steady-state fluorescence spectroscopy was conducted in order to determine the interaction of Que with HP-β-CD and Me-β-CD. The measurements were performed in an Edinburg F5S spectrofluorometer (Edinburgh Instruments Ltd, UK). The excitation and emission slits were set at 5 nm and the emission spectra were recorded using a quartz (1 cm) cuvette, at room

temperature. Que stock solution was prepared in DMSO / distilled water (dH_2O) [50:50 v/v %] at a concentration of 100 μM and kept protected from light. The CD stock solutions were prepared in dH_2O at a concentration of 6 mM. The final concentration of Que in the cuvette was 25 μM for each measurement. Various volumes from the CDs stock solution were added each time (0, 0.1, 0.2 ,0.3 ,0.4 ,0.5 0.6 ,0.7, 0.8 ,0.9, 1.0 ,2.0 ,3.0 ,4.0 and 5.0 mM). The final volume of each sample was 3 mL, adjusted each time with the proper amount of dH_2O. The pH values of the samples were adjusted to 4.5 and 6.8 through the addition of HCl (0.1 M) and NaOH (0.1 M). The samples were kept stirred and protected from light for 30 min, before measurement. The excitation wavelength of Que was set at 375 nm.

The binding constant between Que and each CD was calculated based on the observed emission changes of the fluorescence spectrum upon the addition of different concentrations of 2-HP-β-CD / Me-β-CD. A titration curve at I_{550} was plotted and, by applying linear fitting, the double reciprocal plot of the data was designed (Figures 6, 8). The binding constants were derived from the Benesi−Hildebrand equation:

$$\frac{\mathbf{1}}{\boldsymbol{\Delta F}} = \frac{\mathbf{1}}{\boldsymbol{\Delta F c}} + \frac{\mathbf{1}}{\boldsymbol{K c \Delta F c}[\mathbf{CD}]\mathbf{0}}$$

ΔF represents the difference between the fluorescence intensities in the absence and presence of HP-β-CD/Me-β-CD, K_c is the binding constant, ΔF_c is the difference on intensity between free and complexed Que at 1:1 molar ratio and $[CD]_0$ is the concentration of HP-β-CD / Me-β-CD.

Molecular Dynamic (MD) simulations

The MD simulations were performed with the GPU version of the PMEMD module[18] using the AMBER14 simulation package.[19,20] The geometry of quercetin and methyl-β-cyclodextrin were optimized with the HF/6-31G* basis set (Gaussian09).[21] The General AMBER Force Field (GAFF) was used to obtain force field parameters for quercetin and methyl-β-cyclodextrin with RESP charges.[22,23]

Effect of HP-β-CD and Me-β-CD concentration on the solubility of Que (Phase solubility study)

The effect of HP-β-CD and Me-β-CD on water solubility of pure Que was evaluated at three pH values (1.2, 4.5 and 6.8), using a thermostatic shaking bath (Unitronic orbital J.P. Selecta),[24] with adapted thermostatic unit. More specifically, 15 mg of Que were added into a conical flask. Then, 10 mL of either HCl solution (pH 1.2), or acetate buffer (pH 4.5) or phosphate buffer (pH 6.8) and increasing amounts of HP-β-CD/ Me-β-CD were added to produce cyclodextrin concentrations of 0.004, 0.008, 0.012, 0.016 and 0.02 M. The conical flasks, were placed for 24h equilibration in a shaking bath (37 °C, 50 rpm). After shaking, the samples were filtered with regenerated cellulose filters (Whatman®, Spartan® syringe filters, 0.45 μm), using 1 mL for filters' saturation. The filtered samples were mixed with methanol in a 1:1 ratio for the determination of Que's concentration by UV-Vis. The UV–Vis spectra of phase solubility samples were recorded with a Pharmaspec UV-1700 Schimazdu UV- Vis Spectrophotometer (slit=1, speed 100 nm/min) at room temperature, with medium response speed. The wavelength range was 200-550 nm and the absorption recording range 0.050-1.500 AU. For the calibration curve, 1 mg/mL Que's methanolic stock solution was prepared. Then, it was diluted with water in a 1:1 ratio and appropriate volumes were further diluted with methanol/water solution (50:50 v/v) in order to prepare calibration curve samples ranging from 0.5 μg/mL to 15 μg/mL of Que.

Solubility study of lyophilized Que-Me-β-CD complex

Solubility studies of lyophilized complex of Que with Me-β-CD were also performed, in the same experimental setup, in at three pH values (1.2, 4.5, 6.8), according to the European Medicines Agency (EMA) and the American Food and Drug Administration (FDA) guidelines .[25,26] Specifically, an excess amount (80 mg) of lyophilized Que-Me β-CD complex were mixed with 10 mL of either HCl solution (pH 1.2), or acetate buffer (pH 4.5) or phosphate buffer (pH 6.8). The flasks and the samples were prepared and filtered, respectively, following the same procedure as described in paragraph 2.6. The filtered sample was collected in test tubes and mixed with methanol in a 1:1 ratio. Samples were measured by high performance liquid chromatography (HPLC) with a photodiode array detector (photodiode array, PDA), after appropriate dilutions. HPLC-PDA analyses were performed on a Shimadzu prominence system composed by a LC-20AD Quaternary Gradient Pump with degasser, with an SIL-HT auto-sampler and a photo-diode array detector SPD-M20A. Data acquisition and analysis were performed by LC solution® software. Analysis was carried out on a reverse phase Thermo Aquasil C_{18} column (150×4.6 mm, 5 μm) connected to a guard C_{18} (12.5×4.6 mm, 5 μm particle size) using 0.1% orthophosphate: methanol (35:65), in isocratic mode as mobile phase at 1 $mL \cdot min^{-1}$ flow rate. The injection volume was 20 μL and DAD spectra were acquired with 4 nm resolution in the range 200–400 nm. Sanghavi's et al method[26] was optimized for the needs of the present work and the calibration curve samples ranged from 5 μg / mL to 100 μg / mL of Que. The calibration curve samples were prepared using appropriate volumes of 1 mg/mL Que's methanolic stock solution and mobile phase (65% Methanol – 35% of 0.1% ortho phosphoric acid) for all the dilutions.

***Ex vivo* nasal mucosa permeation experiments**

Rabbit nasal mucosa was selected as permeation tissue for *ex vivo* diffusion experiments[28]. Nasal mucosa was extracted on the day of the experiment from rabbit heads collected from a local slaughterhouse (Athens, Greece). More precisely, a surgical scissor was used in order to cut each nostril in two places on either side of the septum. Ethmoidal air cells were removed with surgical forceps and the parts around the septum were cleaned carefully. Then, the teeth were removed from both sides. Then, the nose bone was cut vertically at the end of the diaphragm (next to the eyes) with the surgical scissors, and the diaphragm was removed. Mucosa was gently isolated from both sides of the septum using a spatula. During the isolation, the mucosa was maintained hydrated with saline solution. After the mucosa's extraction the receptor compartment of Franz-type diffusion cells was filled with PBS (pH 7.4). The excised mucosa was inserted between the donor and receptor compartments of the cell, with the mucosal side facing the donor (cell area: 0.636 cm^2). The assembled system was allowed to equilibrate at 37 °C for 15 min. Then, 25 mg of each test formulation or 15 mg of pure Que were loaded into the donor compartment and wetted with 100 μL of PBS (pH=7.4). The donor and receptor compartments were both covered with parafilm to prevent evaporation. At determined time intervals, 0.5 mL were sampled from the receptor compartment and they were replaced by equal amount of buffer solution (pH=7.4). Que concentration in the samples was measured by the above described HPLC-PDA method and conditions, after appropriate dilution, either immediately or after being frozen at -70 °C until analysis. At the end of the experiment, the amount of formulation left in the donor compartment was quantitatively collected and diluted in order to measure the residual Que and calculate the mass balance. The accumulated drug in the tissue was extracted by comminuting the mucosa with a surgical blade and homogenizing with Ultra-Turrax® IKA (T10 basic model, IKA®-Werke GmbH & Co. KG, Staufen, Germany), in 5 mL of water for 3 minutes (min). Then, it was further homogenized with 2 mL of methanol for 30 more sec. After, the homogenization, the extract was diluted and centrifuged before being measured in HPLC system. Que's amounts recovered from mucosa, receptor and donor compartments allowed for calculating the mass balance.

Statistical Analysis

Data distribution was tested using the Shapiro-Wilk (S-W) normality test. Significance was set at $p < 0.05$ level and all tests were two-tailed with 95% confidence intervals (CI). Results are expressed as mean ± SD. Concentration values were compared statistically between the different pH values and per time point concerning the same pH. Outlier detection occurred by applying the interquartile range (IQR) using a step of 1.5 x IQR. No outliers were detected. The S-W test results revealed that the parameter sets could be considered as Gaussian distributed. Consequently, parametric statistics were applied to confirm whether the differences occurred between the compared groups (e.g. different pH values) were statistically significant. Paired Student's t-test was performed on the obtained values (normally distributed) to detect possible statistically significant differences between the compared groups. Data analysis was performed by SPSS version 25.0 (IBM SPSS Statistics for Windows, Version 25.0, IBM Corporation, Armonk, NY, USA) software package.

RESULTS

Thermal behavior by DSC

The thermodynamic behavior of the HP-β-CD and Me-β-CD, of the drug molecule Que, as well as of their mixtures and lyophilized complexes is presented in Figure 1, while the respective thermodynamic parameter values are enlisted in Table 1.

The CDs exhibited sharp transitions at 167 and 195 °C respectively. This behavior is associated with the physical state and dehydration process of the molecules and shows that in this case, they are more crystalline, compared with amorphous CDs of other studies. Thermal degradation occurred for the molecules above 300 °C .[29-31]
Concerning Que, no heat transfer was observed at 100 °C, indicating that the molecule used in this study was anhydrous.[32-35] The sharp melting peak at 320 °C, as well as the documented transition enthalpy of 115 J/g are both close to the literature data and indicate a slight loss in crystallinity of the drug molecule. However, the T_d and ΔH_d values signify the crystallinity of the molecule.[36] After melting, decomposition occurred.
Based on the rest of the diagrams of Figure 1, we can hypothesize on the interactions between Que and HP-β-CD or Me-β-CD, after physically mixing them or lyophilizing them to form a complex. The melting peak of Que has diminished in all cases and, together with the alteration in the physical state of the CDs, indicates the interaction and possible complexation with Que.[31,32] In the case of the Que:HP-β-CD 1:2 mixture, the interaction broadened the transition, leading to high ΔH_d value. As shown in Table 1, the obtained values for Que-Me-β-CD complex prepared in 1:2 molar ratio are similar with those prepared in 1:1 molar ratio. Based on these results, the Que:Me-β-CD 1:1 molar ratio was selected as the optimum, considering the needed amount and the cost of the raw material, to continue to further experiments.

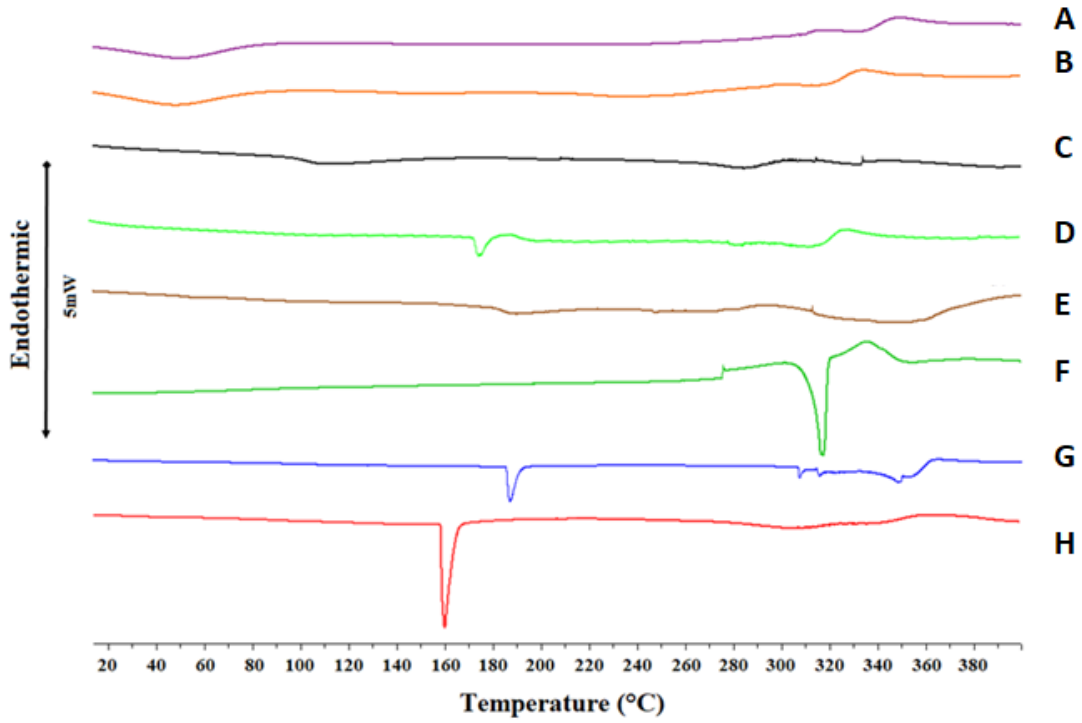

Figure 1: DSC curves of: a) Hydroxypropyl-β-cyclodextrin (HP-β-CD), b). Methyl-β-cyclodextrin (Me-β-CD), c) Quercetin (Que), d) Que:HP-β-CD 1:2 mixture, e) Que:Me-β-CD 1:1 mixture, f) Que:HP-β-CD 1:2 complex, g) Que:Me-β-CD 1:1 complex and h) Que:Me-β-CD 1:2 complex. The double-headed arrow symbol represents a heat flow amount of 5 mW.

Table 1. Thermodynamic parameters of Que, HP-β-CD, Me-β-CD, the physical mixtures of Que with HP-β-CD and Me-β-CD and the respective lyophilized complexes.

Sample	Molar Ratio	$T_{onset,c}$ (°C)	T_c (°C)	$\Delta T_{1/2,c}$ (°C)	ΔH_c (J/g)	$T_{onset,d}$ (°C)	T_d (°C)	$\Delta T_{1/2,d}$ (°C)	ΔH_d (J/g)
HP-β-CD	-	167.09	168.58	3.56	83.06	-	-	-	-
Me-β-CD	-	193.64	194.96	3.12	24.68	-	-	-	-
Que	-	-	-	-	-	315.55	320.10	4.53	115.37
Que:HP-β-CD Mixture	1:2	188.75	197.38	19.96	22.47	316.65	353.10	51.33	214.62
Que:Me-β-CD Mixture	1:1	181.51	182.54	4.18	26.45	304.76	317.94	16.26	35.59
Que:HP-β-CD Complex	1:2	108.94	121.30	22.46	23.78	268.41	289.11	17.89	25.55
Que:Me-β-CD Complex	1:1	31.94	60.89	35.25	93.76	307.53	321.91	16.39	24.72
Que:Me-β-CD: Complex	1:2	31.58	63.89	34.94	89.33	320.82	336.18	15.58	25.16

T_{onset}: temperature at which the thermal event starts; **T:** temperature at which heat capacity (ΔC_p) at constant pressure is maximum; **$\Delta T_{1/2}$:** width at half peak height of the transition; **ΔH**: transition enthalpy normalized per gram of sample. **c:** cyclodextrin or complex transition**; d:** drug molecule transition

High resolution ^{1}H NMR spectroscopy

^{1}H NMR spectra of Me-β-CD, the mixture of Que with Me-β-CD and the respective lyophilized complex, in D_2O at 25 °C are shown in Figure 2. The chemical shifts of the peaks constituting the three spectra are shown in Table 2. Differences between the spectra of the mixture and the complex are observed (Figure 2 and Table 2) signifying the complexation between Me-β-CD and Que with the procedure used

Table 2. ^{1}H NMR chemical shifts for Que, Me-β-CD and the lyophilized complex, in D_2O at 25 °C.

Protons	Me-β-CD	Que	Complex
H_3,H_4,H_5,H_{6a},H_{6b}	3.60-4.00 (bp)		3.60-3.96 (bp)
6' (Que)		8.48 (s)	8.05 (s)
2' (Que)		7.71(bs)	7.68 (d)
3' (Que)		7.66(d)	7.62 (d)
8 (Que)		7.07 (d)	7.05(s)
6 (Que)		6.54-6.30(bs)	6.62 (s)
Anomeric protons	5.09(s),5,30(s)		5.05(s),5,27(s)
Methoxy group	3.41(s)		3.40(s)

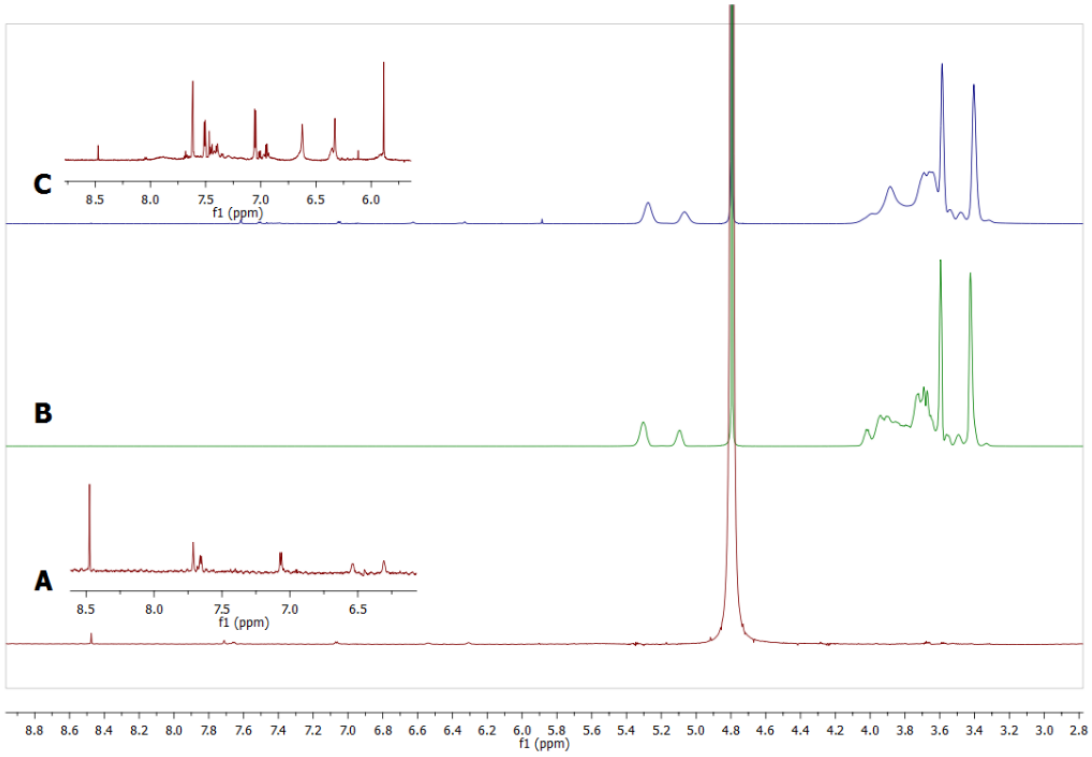

Figure 2: The ^{1}H NMR of (A) complex of Que with Me-β-CD (B) Me-β-CD (C) mixture of QUE with Me-β-CD. The spectra were obtained at 25 °C in D_2O.

The complexation of QUE with Me-β-CD is also illustrated with a 2D DOSY experiment where the diffusion coefficient for the complex is found to be $2.3.10^{-10}$ m^2s^{-1} (Figure 3 A), while in the 2D NOESY spectrum strong cross-peaks between all aromatic protons of Que and ring

hydrogen atoms of Me-β-CD ranged between 3.6-4.0 ppm, as well as with methoxy groups were recorded (Figure 3B) (Table 3).

Table 3. 2D NOESY cross-peaks between Me-β-CD and Que.

6',2',3',8,6, (QUE) -Methoxy group	8.48,7.71,7.66,7.07,6.54 -3.41
6',2',3',8,6, (QUE)-H3,H4,H5,H6a,H6b	8.48,7.71,7.66,7.07,6.54 -3.60,3.96

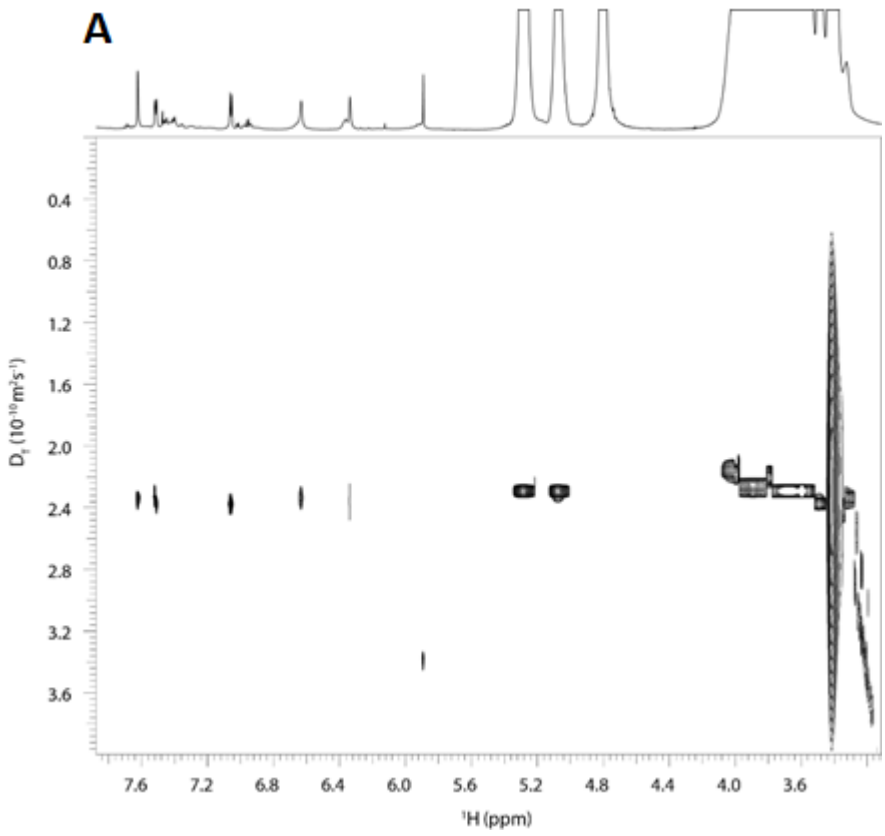

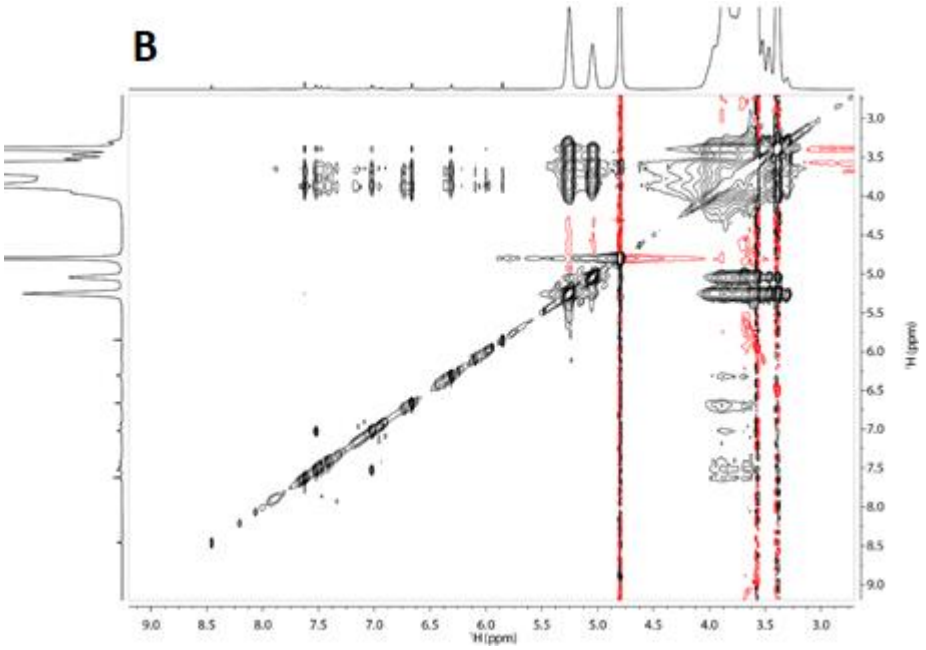

Figure 3: (A): The 2D DOSY experiment of the complex of QUE with Me-β-CD. The spectrum was obtained at 25° C in D_2O. (**B**): The 2D NOESY experiment of the complex of QUE with Me-β-CD. The spectrum was obtained at 25° C in D_2O and using mixing time of 800 ms.

Comparison of the obtained data with those reported by Min Liu et al.[36] show mostly similarities and few differences. This is expected as the authors used D_2O/DMSO (V:V=6:4) mixture in their studies and not pure D_2O. Their system provided the possibility to estimate Δδ=δ(complexation)-δ(quest). However, in our case Δδ= δ(complexation)-δ(mixture) as δ(quest) could not be estimated since Que was insoluble in D_2O. The trends of Δδ were identical in both systems for 2', 6' and 6 protons and differed only at protons 8. However, the conclusions were consistent, thus the hydrophobic part of Que interacted with the hydrophobic cavity of the CDs. This conclusion is also derived using MD calculations as it is described below.

Fluorescence Spectroscopic Studies

In order to evaluate the interaction between Que and CDs, fluorescence spectroscopy was performed. The fluorescence signal of a small molecule can be modified upon the encapsulation in the cavity of a supramolecule such as CD.[38,39]The spectroscopic behavior of Que was investigated by adding increasing concentrations of either HP-β-CD or Me-β-CD into a stable concentration solution of Que.

Upon the gradual addition of the 2-HP-β-CD the fluorescent signal of the Que-HP-β-CD physical mixture was enhanced. The relative fluorescence intensity was increased dramatically, as it exhibited a final 4.8 and 3.2-fold raise in the presence of 5 mM of HP-β-CD (Figure 4A, B) at pH 4.5 and 6.8 respectively. The fluorescence enhancement is usually observed, when a small molecule interacts with CD due to the changes occurring in the microenvironment of the small molecule upon encapsulation.[40-42] The quantum yield of Que rises leading to a higher fluorescence intensity as it is transferred from the aqueous solution into the hydrophobic cavity of 2-HP-β-CD. The interaction of Que with 2HP-β-CD was calculated as described above by applying Benesi−Hildebrand equation (Figure 5). The straight line of the double reciprocal plot confirms the 1:1 stoichiometry of Que with HP-β-CD, and the binding constants were calculated equal to 576 M^{-1} and 824 M^{-1}, at pH 4.5 and 6.8 respectively, indicating a moderate affinity between the two molecules, which is in agreement with the estimated values of similar interactions[6].

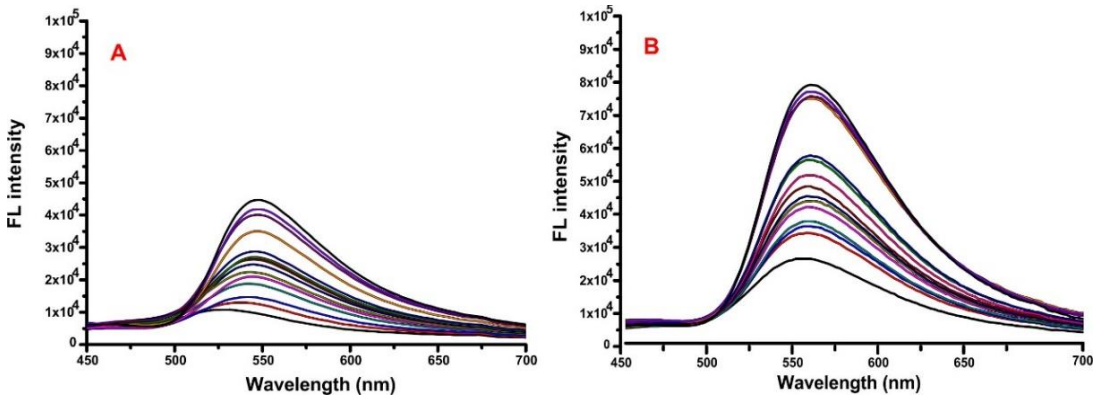

Figure 4: Fluorescence spectra of Que after titrating with various concentrations of 2-HP-β-CD (0, 0.1, 0.2 ,0.3 ,0.4 ,0.5 0.6 ,0.7, 0.8 ,0.9, 1.0 ,2.0 ,3.0 ,4.0 and 5.0 mM) at pH 4.5 (A) and 6.8 (B), respectively.

In a very similar way, upon the gradual addition of Me-β-CD, the fluorescence signal was enhanced by 3.9 and 2.6-fold rise at pH 4.5 and 6.8, respectively (Figure 6 A, B and Figure 7). The straight line of the double reciprocal plot confirms again the 1:1 stoichiometry of Que with Me-β-CD while the binding constants were equal to 1160 and 974 M^{-1} at pH 4.5 and 6.8, respectively, indicating a stronger affinity between the two molecules compared to the interaction of Que with HP-β-CD.

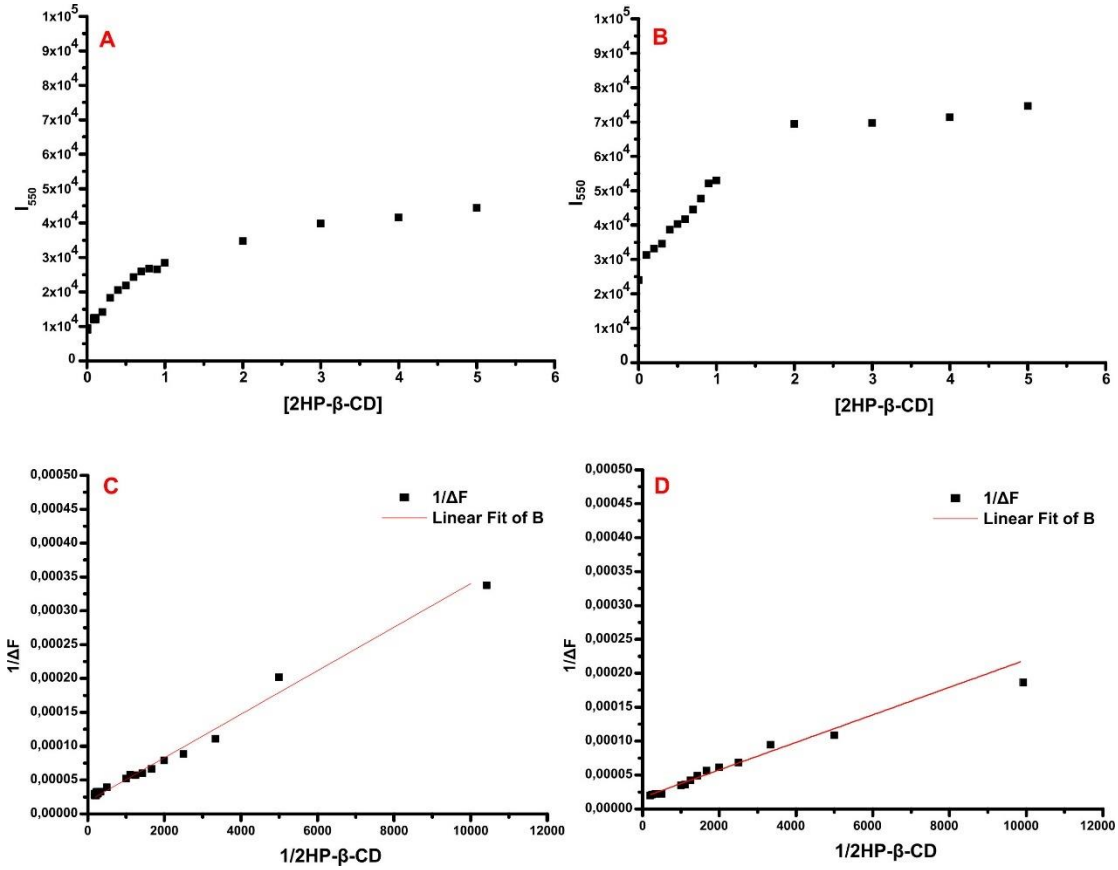

Figure 5: I_{550} of Que after the titration with various 2HP-β-CD concentrations (0, 0.1, 0.2, 0.3, 0.4, 0.5 0.6, 0.7, 0.8, 0.9, 1.0, 2.0, 3.0, 4.0 and 5.0 mM) at pH 4.5 (A) and 6.8 (B), respectively. C and D represent the double-reciprocal plots as they were derived from the data of A and B, respectively.

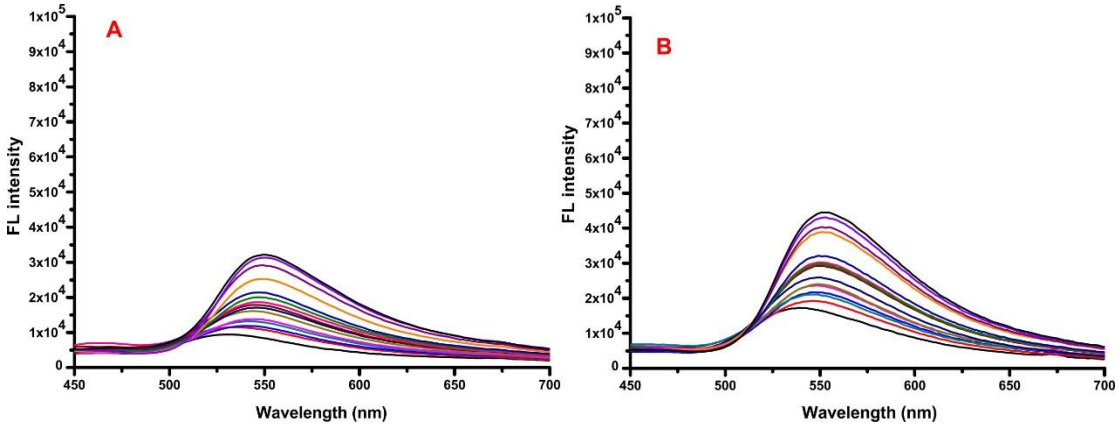

Figure 6: Fluorescence spectra of Que after the titration with various Me-β-CD concentrations (0, 0.1, 0.2 ,0.3 ,0.4 ,0.5 0.6 ,0.7, 0.8 ,0.9, 1.0 ,2.0 ,3.0 ,4.0 and 5.0 mM) at pH 4.5 (A) and 6.8 (B), respectively.

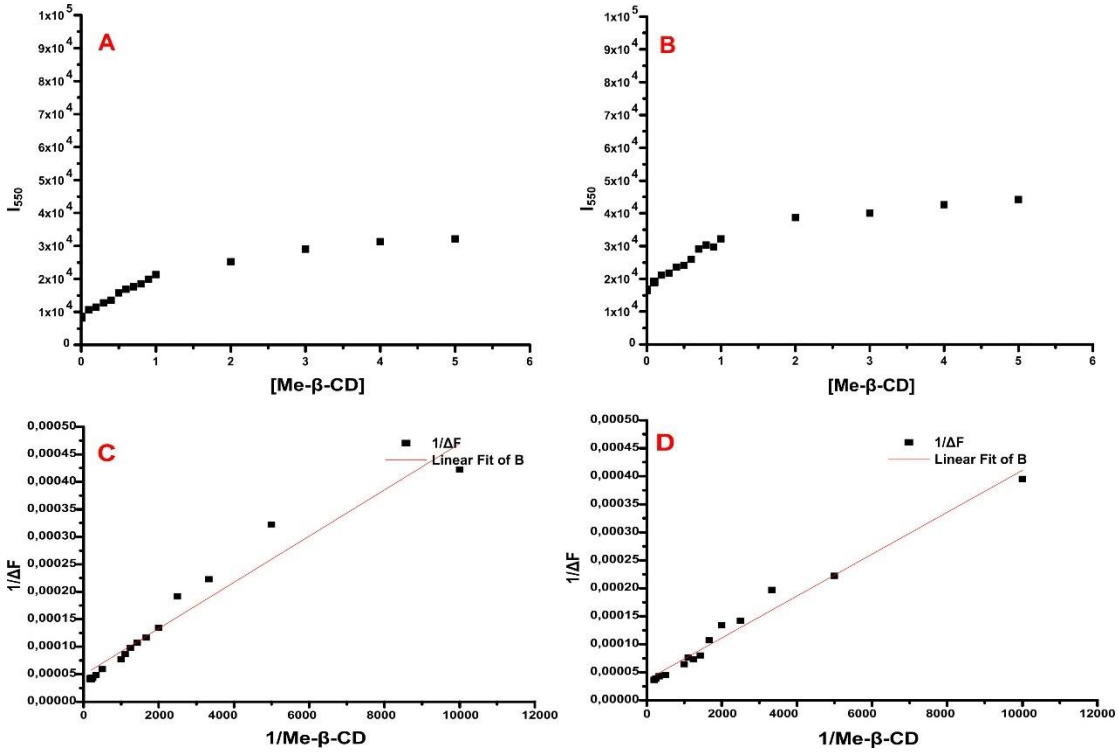

Figure 7: I_{550} of Que after the titration with various Me-β-CD concentrations (0, 0.1, 0.2, 0.3, 0.4, 0.5 0.6, 0.7, 0.8, 0.9, 1.0, 2.0, 3.0, 4.0 and 5.0 mM) at pH 4.5 (A) and 6.8 (B), respectively and D represent the double reciprocal plots as they were derived from the data of A and B, respectively.

Molecular Dynamics (MD) simulations

In order to describe the possible position of Que inside the Me-β-CD cavity we conducted MD simulations and compared the results with previously reported data for the interaction of Que with HP-β-CD.[8] Figure 8 shows the results from these MD simulations. The hydrophobic segment of Que is inserted into the Me-β-CD cavity with the hydrophobic interactions prevealing to the complex formation, in a similar maner as with HP-β-CD. However, further simulations will be required to derive the thermodynamic parameters of the binding and reveal whether the complexation of Que with Me-β-CD is energetically favorable as is the case of Que complexation with HP-β-CD.[8]

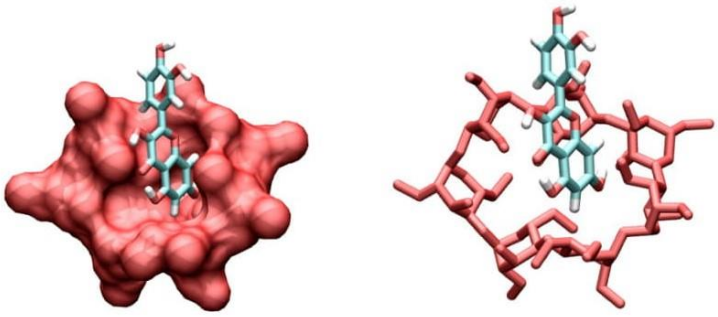

Figure 8. The complex of quercetin and methyl-β-cyclodextrin as it derived from the MD simulations. At the left part of the figure emphasis is given in the cavity where the hydrophobic segment of quercetin is embedded while in the right emphasis is given in the details of the interactions between the two molecules.

Effect HP-β-CD and Me-β-CD concentration on the solubility of Que in water

HP-β-CD: From Figure 9A, we conclude that the water solubility of Que is significantly increased when added concentrations of HP-β-CD are also increased. In particular, the highest increase was observed at pH 6.8, while the smallest enhancement occurred at pH 1.2. Basically, at pH 1.2 and 4.5, HP-β-CD appears to bear a similar effect, slightly increasing the water solubility of Que. At pH 6.8, Que's solubility increases linearly up to a concentration of cyclodextrin equal to 0.012 M (R^2=0.9734) and then it positively deviates linearity (R^2=0.87 for all the time points). This fact probably indicates the formation of a complex involving more than one molecule of cyclodextrin.[24] On the contrary, at pH 1.2 and 4.5 the correlation between "Que concentration- cyclodextrin concentration" is linear over the whole range of HP-β-CD concentrations used in this study (R^2=0.928 and 0.960 at pH 1.2 and 4.5, respectively).

Me-β-CD: As shown in Figure 9B, in the presence of Me-β-CD, water solubility of Que was increased at a higher extent at pH 6.8 than at pH 4.5 and 1.2, respectively ($p<0.05$, 95% CI). In this study, at all pH conditions, Que concentration increased linearly with increasing molecular concentration of added Me-β-CD (R^2 0.960, 0.950, 0.977 at pH 1.2, 4.5 and 6.8, respectively). Comparing the effect of the two β-CDs on the water solubility of Que, both CDs achieve similar final Que concentration at pH 6.8 despite the possible different stoichiometry of the produced complex in the presence of HP-β-CD, as revealed by the respective phase solubility diagram (Figure 9A). At pH 1.2, the solubility of Que in the presence of Me-β-CD is increased compared to the one in the presence of HP-β-CD ($p<0.05$, 95% CI), most likely, due to the increased lipophilic character of Me-β-CD, because of the substitution of β-CD hydroxyl groups by methyl groups. This structural difference, may favor the formation of an inclusion complex with the molecules of non-ionized Que, which predominate in acidic pH conditions. Overall, Que was found to be more soluble at pH 1.2 compared to pH 4.5 in the presence of Me-β-CD while Que solubility is similar in both pH values in the presence of HP-β-CD.

The linear relationship revealed between Que concentration and the concentration of both CDs used in the present study, enabled the calculation of the binding constants for the formed inclusion complexes at all pH conditions considered. The calculated values are presented in Table 4 and they are approximately half of those calculated by the double reciprocal plot of the fluorescent study. This is probably attributed to the different methodologies applied in the two experiments, using different CD and Que concentration ranges. More specifically, the CD concentration ranged from 0-5.0 mM and from 0-20mM in the fluorescence experiment and the phase solubility experiments, respectively, while, Que concentration was kept constant (100 μM) in the fluorescence experiment and ranged from almost zero to 100 μM and 400 μM at pH 4.5 and 6.8, respectively. Furthermore, the different dissolution media used in the two experiments (water in phase solubility and water/DMSO in fluorescence experiments) may also contribute to the differences observed in the estimated binding constants.

Table 4. Summary of the estimated binding constants of Que complexes with HP-β-CD and Me-β-CD at pH 1.2, 4.5 and 6.8.

pH	$K_{Q\text{-}HP\text{-}\beta\text{-}CD}$ (M^{-1})	$K_{Q\text{-}Me\text{-}\beta\text{-}CD}$ (M^{-1})
1.2	609 ± 21	491 ± 27
4.5	378 ± 19	627 ± 154
6.8	570 ± 105*	636 ± 101
*Calculation of K based on the initial linear part of the phase solubility diagram (Figure 10)		

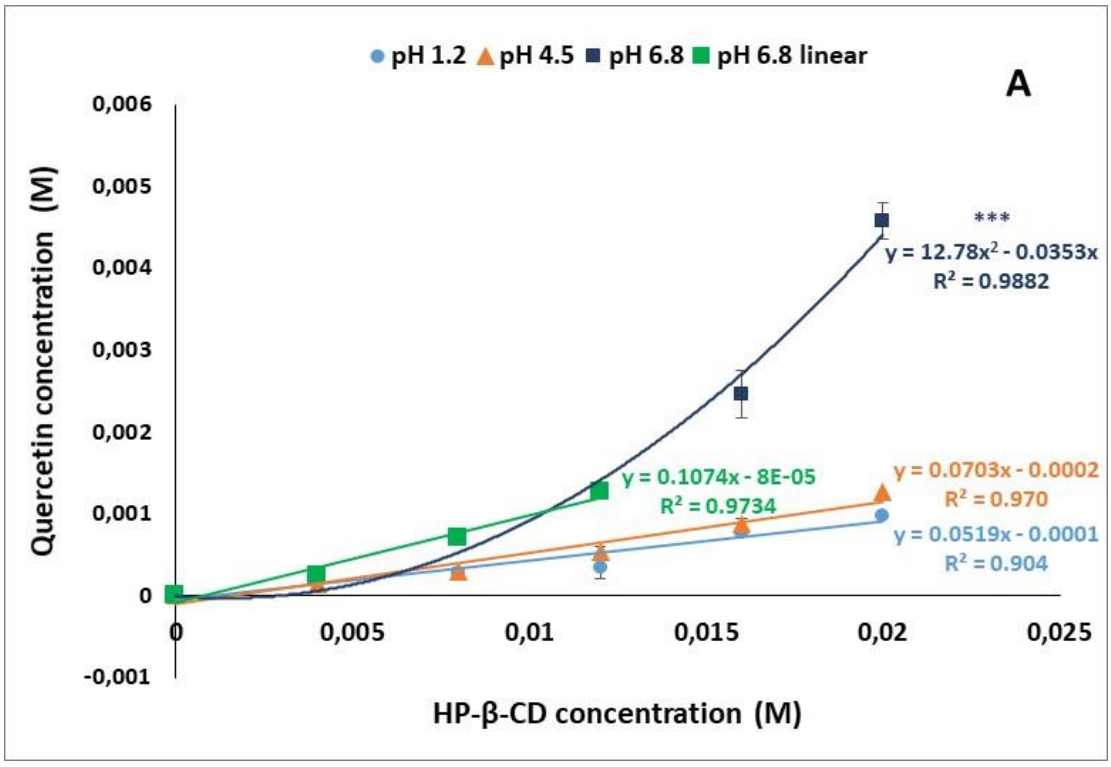

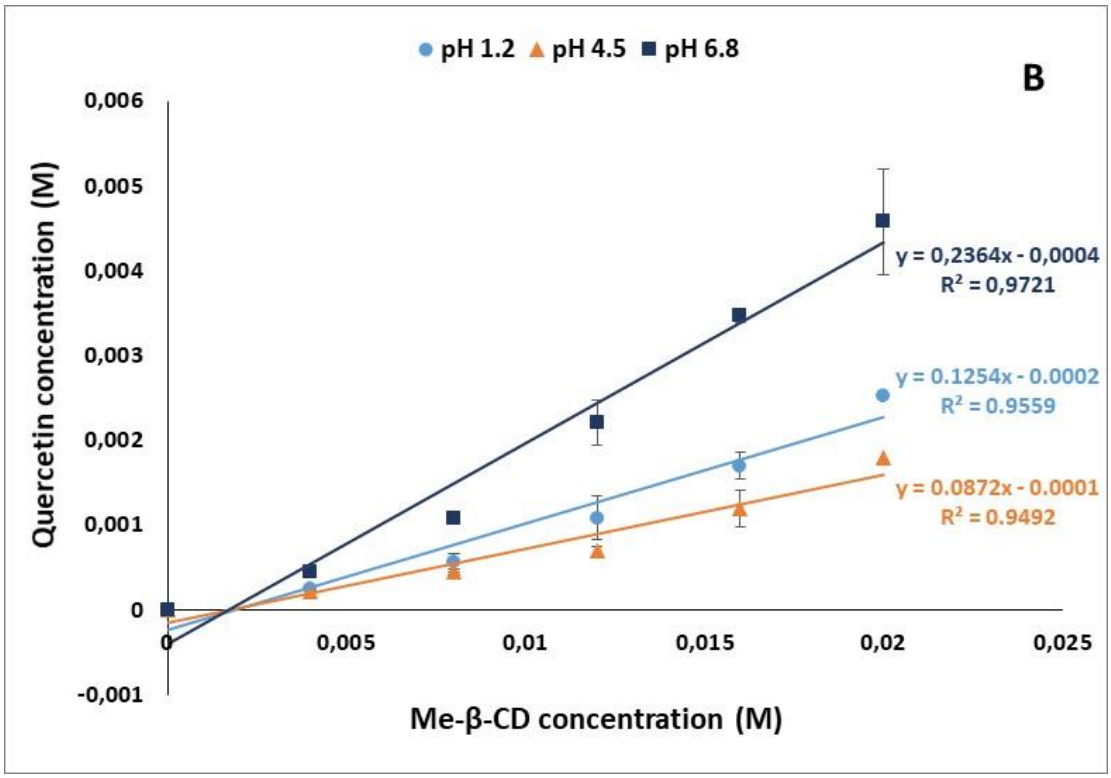

Figure 9: (A) Effect of HP-β-CD and pH on the water solubility of pure Que. (*** Possible formation of a complex involving more than one molecule of cyclodextrin). **(B)** Effect of Me-β-CD and pH on the water solubility of pure Que. Water solubility of Que was found significant greater at pH 6.8 than in 4.5 and 1.2, respectively ($p<0.05$, paired Student's t-test)

Solubility study of lyophilized Que-Me-β-CD complex

HPLC determination revealed 13.7% (w/w) content of Que in the Que-Me-β-CD complex. The results illustrated in Figure 10 show that after 3 h of equilibration in the thermostatic shaking bath at 37 °C, Que's concentration reaches its maximum at all pH values, and thereafter, a gradual decrease of measured concentration is observed at all time points and for a total time of 48 h. This is most likely attributed to the dissociation of the complex and precipitation and/or degradation of free Que. More specifically, the maximum measured Que concentration was found 0.165 ± 0.005 mg/mL and 0.164 ± 0.011 mg/mL after 3 h at pH 1.2 and 4.5, respectively, and 0.228 ± 0.002 mg/mL after 6 h at pH 6.8, values that could be considered as saturation solubility of Que in different pH conditions. These values declined to 0.080 ± 0.001 mg/mL at pH 1.2, 0.084 ± 0.001 mg/mL at pH 4.5 and 0.110 ± 0.001 mg/mL at pH 6.8 after 48 h.

According to the HPLC chromatograms, the hypothesis of Que's degradation even from the first time point seems reasonable, because, apart from the main peak of Que eluted at 2.6 min, a second peak (probably degradation peak) was also observed at all time points, with retention time 6.27 min at pH 1.2 and 4.5 and 3.9 min at pH 6.8, where a third degradation peak was also observed (retention time 3.3 min), probably indicating the production of more and/or different degradation products, in these pH conditions. The areas' ratios (degradation peak area/Que area ratio) increase with the time for pH 1.2 and 4.5 (0.6-1.4 and 0.5-11.3, respectively), but not at pH 6.8 (degradation peak area/Que area ratio: 0.1-0.3), probably due to the simultaneous presence of more than one degradation products. It worthy to note that these observations are consistent with the MD simulations where we observed in the trajectory this "dissociation-complexation through time" and in a subsequent study devoted solely on MD calculations, we will discuss in details this issue.
The results of this study were also compared with those recently reported by Diamantis et al. (2018) for the solubility of pure Que and its lyophilized product with HP-β-CD (Table 6).[9]

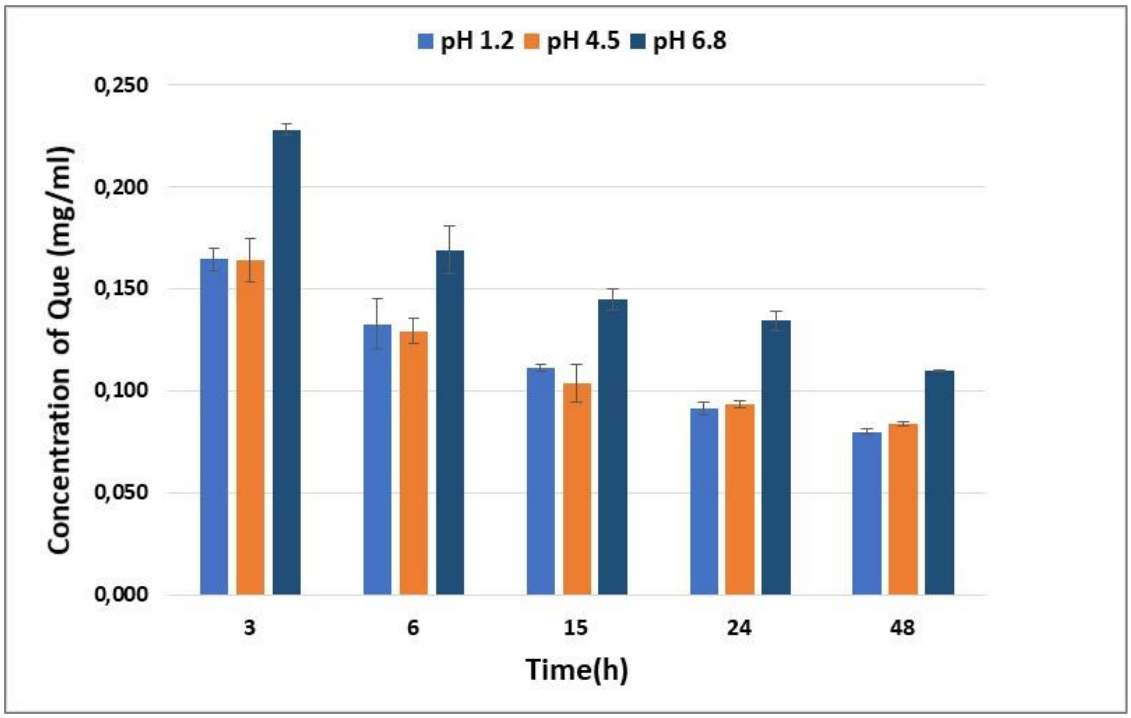

Figure 10: Effect of pH on the solubility of Que-Me-β-CD lyophilized complex. (* Water solubility of Que-Me-β-CD lyophilized complex was found significantly greater at pH 6.8 than in 4.5 and 1.2, at all-time points ($p<0.05$, paired Student's t-test).

Ex vivo nasal mucosa permeation experiments

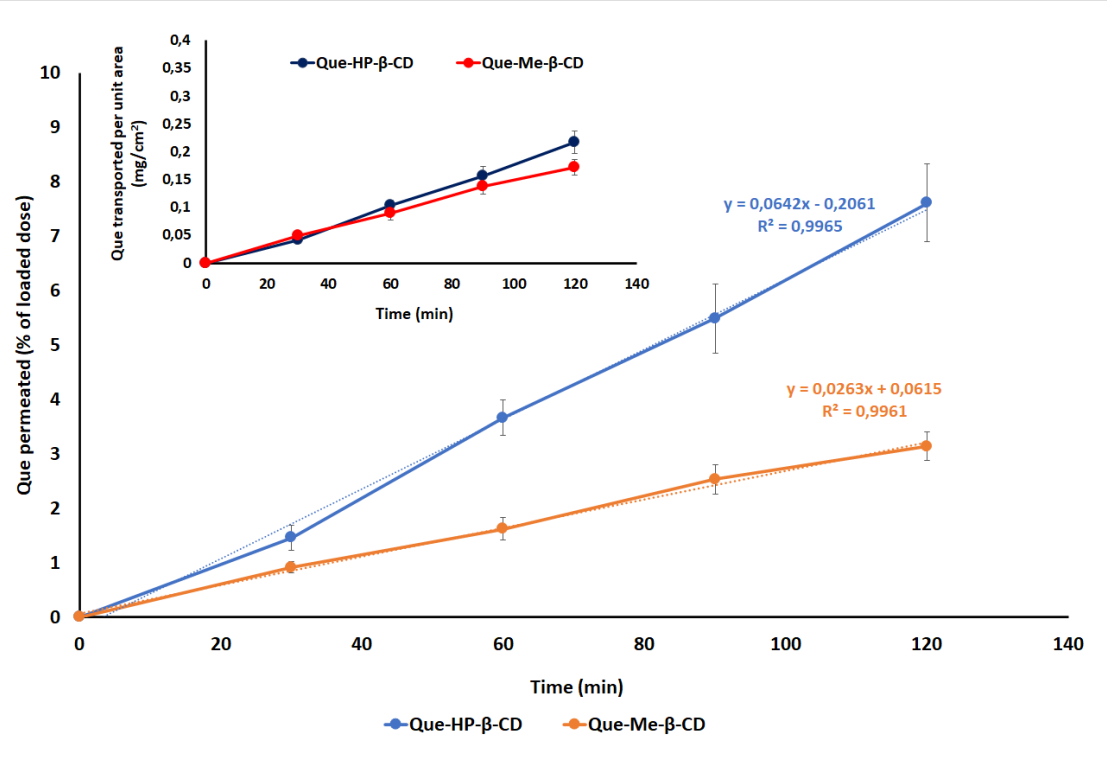

Figure 11. : Permeation profiles across rabbit nasal mucosa of Que-HP-β-CD and Que-Me-β-CD lyophilized formulations, expressed as % of the loaded dose (mean ± SEM) vs time, for 2 h experiments (n=6) and cumulative Que amount permeated per unit area Vs time (Insert graph)

Ex vivo experiments, using rabbit nasal mucosa as permeation barrier, lasted 2 hours (h). Preliminary experiments lasting 4 h were performed as well. Based on the Que's content in the lyophilized powders, the 25 mg of powder loaded, contained a dose of Que of 1.80 mg and 3.48 mg for Que-HP-β-CD and Que-Me-β-CD, respectively. Figure 11 reveals that until the first time point (30 min) the permeation is not significantly different between the two lyophilized powders ($p>0.05$, 95% CI). At all the other time points until the end of the experiment, as far as the percentage of the loading dose permeated is concerned, Que-HP-β-CD presents significantly better permeation profile ($p<0.05$, 95% CI). The permeation profile is linear in both cases, indicating the maintenance of sink conditions at all time points (R^2=0.9965 and R^2=0.9961 for Que-HP-β-CD and Que-Me-β-CD, respectively). Sink conditions are also maintained after 4 h, as it arises from the preliminary experiments. The maximum values of permeation are obtained after 2 h and they are presented in Table 5. When looking at the amount of Que permeated per unit area (insert graph in Figure 11), it is observed that Que-Me-β-CD and Que-HP-β-CD present similar permeation profile at all the time points of the experiments. The permeation profile of pure Que is not presented in Figure 11, as the amount of Que permeated during the experiment was negligible at all the time points.

Table 5. Permeation values for Que-HP-β-CD and Que-Me-β-CD lyophilized powders after 2 h, expressed as % loading dose and amount of Que permeated per unit area

Time point: 2h	**Que-HP-β-CD**	**Que-Me-β-CD**
% of loaded dose	7.61 ± 1.76	3.14 ± 0.63
mg/cm^2	0.22 ± 0.05	0.17 ±0.04

DISCUSSION

The direct drug transfer from the nasal cavity to CNS is accomplished via the olfactory region achieving blood-brain barrier (BBB) shortcut. Intranasal delivery is a very promising route of administration, however nasal transmucosal absorption is affected by the physicochemical properties of the drugs and formulation factors.[43,44] As the volume of nasal fluids is restricted, solubility is a major factor which influences the rate and the extent of nasal drug absorption. The development and evaluation of solid candidate formulations for nasal delivery requires them to be soluble in various pH values, because their permeability from the nasal olfactory region depends mainly on the amount of dissolved drug in the cavity[44]. In addition, the pH of the nasal mucosa varies from 5.5-6.7 in normal situations and it can be more basic or acidic in case of chronic disease.[2]

In the present study we used Me-β-CD to enhance Que's solubility by the formation of inclusion complex, as in the previously prepared inclusion complex of Que with HP-β-CD,[9] in order to be utilized as possible carriers for Que's intranasal administration and nose-to-brain Que delivery.

The formation of Que inclusion complex with Me-β-CD, in comparison to the Que-HP-β-CD, was investigated and confirmed by biophysical methods. ^{1}H NMR spectra of Me-β-CD, Que and the lyophilized complex of Que with Me-β-CD in D_2O at 25 °C, in conjunction with 2D NOESY and 2D DOSY experiments revealed strong interaction between Que and Me-β-CD[42-49], stronger than those previously reported between Que and HP-β-CD.[8,9] More specifically, 2D NOESY spectra showed strong correlations between Me-β-CD and Que molecules, while the observed chemical shift changes, due to the complex formation, provide information on their molecular interactions occurring between all aromatic protons of Que and ring hydrogen atoms of Me-β-CD, as well as with methoxy groups (Figure 3, Tables 2,3). In parallel, 2D DOSY experiment enabled the determination of self-diffusion coefficients and confirmed the intermolecular interactions of Que with Me-β-CD. Furthermore, fluorescence spectroscopy (Figures 5-8), revealed 1:1 interaction of both HP-β-CD and Me-β-CD with Que, while Me-β-CD was found to exhibit higher affinity for Que than HP-β-CD at pH 4.5 and 6.8 that were used to simulate the physiological pH range of nasal cavity. Preliminary MD simulations also confirmed the inclusion of Que into the Me-β-CD cavity, as was previously reported also for the complexation of Que with HP-β-CD.[8] In addition these preliminary results point out that complexation is time dependent and transient dissociation is occurring during the trajectory. Detailed study discussing this observation and the complexation: dissociation aspects will follow in a subsequent study.

The effect of β-CD derivatives in Que's solubility and the determined aqueous solubility of the prepared Que-Me-β-CD lyophilized product, tested at three different pH values, proves the greater solubility of Que upon complexation with CDs as the pH increases. These results favor the preparation of nasal powders which should being dissolved in the acidic conditions of nasal cavity, where the pH of nasal fluids vary from 4 to 6.5. According to the literature, it is quite difficult to conclude a certain value of acidity constant for Que because a significant variation ranging from 3.5 to 8.2 is reported. The most dominant value is 7.1 ± 1.2. In order to better understand the solubility profile in different pH values, it is important to overview the acidity character of particular hydrogens in the polyphenolic structure of Que. The correct

determination of deprotonation in the presence of strong or weak basic conditions is not an easy task and a limited number of publications is reported. In general, it can be said that the addition of a strong base (e.g. sodium methoxide) ionize all hydroxyl groups in Que's structure, whereas the addition of a weaker base (sodium acetate) cause the ionization of only three protons at positions 3,7,4' (Scheme 2).[50] Considering the possible ionization forms of Que in the current pH conditions of the solubility experiments, at pH 1.2 Que is not ionized at all, but at pH 4.5 a great amount of Que molecules is ionized. In the presence of CH_3COO^-, these molecules lose the three protons at positions 3,7,4', as mentioned above and as the pH reaches the pKa value (pKa= 7.1 ± 1.2), forms A and B exist equally in the solution. Presence of form C could be considered negligible in the pH range of our study since OH at position 5 makes a very strong hydrogen bond with the neighboring carbonyl group.

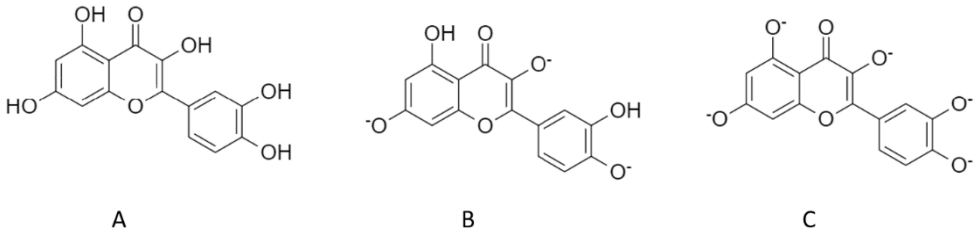

Scheme 2: A) Structure of Que, B, C) Deprotonated forms of Que.

The degree of molecule's ionization demonstrates an important role in the possible interactions developed in the lipophilic cavity of CD. The deprotonated substances are more hydrophilic, so their complexation with the hydrophobic CD cavity is less favored.[51] This fact, explains also the greater binding constant at pH 4.5 as it was determined by the fluorescence spectroscopic studies (1160 M^{-1} at pH 4.5 and 974 M^{-1} at pH 6.8). Although the constants differ, in the phase solubility study we noticed greater values of measured Que at pH 6.8, probably due to the contribution of the higher solubility the free Que at this pH. Furthermore, the deviation from linearity of the phase solubility diagram at pH 6.8, mainly in case of HP-β-CD (Figure 9A), is an indication for a second 1:2 (Que:CD) complex formation.[24] The substitution of β-CD with methyl groups, in case of Me-β-CD, does not permit this interaction as it can hypothesized from the Figure 10. The calculated association constant, K, values at different pH conditions for both CDs are given in Table 4. At pH 6.8, the presented value for the interaction of Que with HP-β-CD, is calculated taking into account only the initial linear part of the phase solubility diagram (Figure 9). The K values show that the potency of the formed complex is similar for the two CDs and does not change significantly in the studied pH range. These results are consistent with previous published work conducting phase solubility experiments in similar concentrations and pH conditions[35]. Discrepancies cited in the literature are probably attributed to the different experimental conditions used (e.g. pH and temperature)[34] or the different method for calculation of binding constants[37].

Subsequently, Table 6 presents the solubility's results of the lyophilized product of Que with Me-β-CD at pH 1.2, 4.5 and 6.8, in correlation with the solubility's results of pure Que and the lyophilized product of Que with HP-β-CD at pH values mentioned above, in the same conditions, as they were determined in a previous study.[9] Regarding Que-Me-β-CD, the difference in measured Que's concentration, at pH 1.2 and 4.5, is not statistically significant ($p>0.05$, 95% CI). The greatest value was obtained at 3 h, at pH 6.8 and differs significantly with those at pH 1.2 and 4.5 ($p<0.05$, 95% CI). Among the different time points we, also, observed a significant decrease ($p<0.05$, 95% CI), which reflects Que's degradation as the residence time in shaking bath increases.

Regarding the Que-HP-β-CD lyophilized complex, Diamantis et al.[9] found Que's solubility significantly greater at pH 6.8 and lower at pH 4.5 and 1.2, as it was expected according to literature (quercetin pK_a = 7.1±1.2, so at pH 6.8, quercetin is ionized by 50%).[48] The lyophilized product Que-HP-β-CD was approximately 15-50 times more soluble than pure Que in different pH conditions. Similarly, in the present study, concerning the complex of Que with Me-β-CD, the highest solubility for Que was found at pH 6.8 and the complex seems to be approximately 6-40 times more soluble than pure Que in different pH conditions. The observed differences between the two lyophilized products, are likely due to the different physicochemical properties of CDs (ex. molecular weight, water solubility, lipophilicity). HP-β-CD is more soluble at pH 6.8 forming hydrogen bonds in the water environment, in opposition to Me-β-CD. At pH 1.2 and 4.5 Me-β-CD surpass HP-β-CD as more lipophilic.

Table 6. Solubility of pure Que and its lyophilized products with HP-β-CD and Me-β-CD at pH 1.2, 4.5 and 6.8.

	pH	Solubility (mg/mL) ± SD	Solubility ratio lyophilized product/Que
Que[#]	1.2	0.004±0.001*	
	4.5	0.004±0.001*	
	6.8	0.016±0.004[$$]	
Que-HP-β-CD[#]	1.2	0.19±0.07** - 0.07±0.04***	47.5 – 17.5
	4.5	0.13±0.,02** - 0.085±0.004	32.5 – 21.25
	6.8	0.47±0.117[$] - 0.23±0.03[£]	29.38 – 14.38
Que-Me-β-CD	1.2	0.16±0.01[$] - 0.08±0.00[$$]	40 – 20
	4.5	0.16±0,03[$]- 0.08±0.00[$$]	40 – 20
	6.8	0.23±0.01[$] – 0.11±0.00[$$]	14.37 – 6.87

*mean of 3, 6, 15, 24, 48 h; **mean of 3, 6, 15 ;, ***mean of 24, 48 h, [$]mean of 3 h; [$$]mean of 48 h; [£]Concentration measured (mean ± SD) at 15, 24 and 48 h of experiment; [#] from ref.[9]

Literature references[9,52-54] classify Que either as class II or class IV drug (either highly permeable-poorly soluble or poor permeable-poorly soluble), according to Biopharmaceutics Classification System.[55,56] This fact implies that drug's main absorption carried out via aqueous diffusion. Cyclodextrins could enhance the permeation of drugs whose rate-limiting step is the permeation through aqueous diffusion layer. The administrated powder could act as depot formulation and at this point further research is ongoing to scrutinize the analogy among the diffusion and solubility rate. Moreover, Me-β-CD, as lipophilic compound, interacts with biological membranes increasing more efficiently the absorption**.** This is one reason why it is one of the most commonly studied cyclodextrin in nasal drug delivery.[57]

Ex vivo permeation experiments showed that the presence of cyclodextrins enabled Que's permeation across the nasal mucosa barrier. Pure Que could not be absorbed in the nasal cavity as it could not be dissolved in the available volume of fluid in the donor compartment simulating nasal fluids (100 μL) due to its limited aqueous solubility. In contrast, an increasing amount of Que was found to permeate across the nasal mucosa from both Que-HP-β-CD and Que-Me-β-CD lyophilized powders (Fig. 11). Furthermore, despite the different loading dose of Que in the two powders, the amounts of Que diffused in the receptor compartment after 2 h were not significantly different (0.14 mg and 0.11 mg for Que-HP-β-CD and Que-Me-β-CD, respectively). This is probably due to the greater aqueous solubility observed in the case of Que-HP-β-CD lyophilized powder (Table 6) that is compensated by the the interaction of Me-β-CD with the nasal epithelial membranes, transiently open tight junctions and increase Que's permeation, in the case of Que-Me-β-CD lyophilized powder.[58]

According to literature, Que is not able to cross the blood brain barrier after its absorption through the gastrointestinal tract. More precisely, oral administration of Que in rats, resulted

in negligible amounts (< 0.00001 % of the loading dose), in the brain.[59] Therefore, the permeation values obtained from *ex vivo* experiments in our study, encourage the future *in vivo* evaluation of nasal administration of the lyophilized products of Que with HP-β-CD and Me-β-CD, using appropriate animal models. We intend to proof Que's nose-to-brain delivery and determine a possible nasal therapeutic dose.

CONCLUSIONS

In conclusion, inclusion complexes of Que with HP-β-CD and Me-β-CD were prepared, and their formation was validated through DSC thermograms, as well as through NMR and fluorescence spectroscopy experiments, revealing strong interaction and a 1:1 complex. In the phase solubility studies, a linear increase in Que's solubility with increasing CD concentration was observed in the entire range of pH conditions studied. The positive deviation from the linearity, observed mainly in HP-β-CD at pH 6.8, can be probably attributed to further formation of a 1:2 (Que-CD) complex.[24] The aqueous solubility of the lyophilized products of Que with Me-β-CD and HP-β-CD was found to be 40 and 50 times higher than that of pure Que, respectively. The preliminary *ex vivo* permeation experiment from rabbit nasal mucosa revealed measurable and similar Que permeability profile with both CDs and negligible permeation of pure Que. The solubility and permeability behavior of the lyophilized products encourage the formulation of nasal powders able to dissolve and release Que through nasal mucosa, and probably also achieve nose-to-brain delivery. This is also supported by the calculated binding constant values indicating a complexation which permits drug delivery through a biological membrane (< 10^3 M^{-1}). Further research is ongoing for their ex-vivo and *in vivo* evaluation for nasal administration and nose-to-brain delivery.

Acknowledgments: Prof. Thomas Mavromoustakos (TM) acknowledges CERIC supporting funding for performing the experiments in NCI of Lubljuana, Slovenia.

Conflicts of Interest: The authors declare no conflict of interest.

REFERENCES

1. Wang, J.; Zhao, X.H. Degradation kinetics of fisetin and quercetin in solutions affected by medium pH, temperature and co-existing proteins. *J.Serb. Chem. Soc.*, **2016**, 81 (3), 243–253.
2. Kim, B.H.; Choi, J. S.; Yi, E.H.; Lee, J. K.; Won, C.; Ye, S. K.; Kim, M.H. Relative antioxidant activities of quercetin and its structurally related substances and their effects on NF-kB/CRE/AP-1 signaling in murine macrophages. *Molecules and Cells*, **2013,** 35, 410-420, doi: 10.1007/s10059-013-0031-z.
3. Valko, M.; Rhodes, C. J.; et al. Free radicals, metals and antioxidants in oxidative stress-induced cancer. *Chem.-bio. int.*, **2006**, 160, 1-40.
4. Cai, X.; Fang, Z.; et al. Bioavailability of Quercetin: Problems and Promises. *Cur. Med. Chem.*, **2006**, 20(20), 2572–2582.
5. Gao, L.; Liu, G.; et al. Preparation of a chemically stable quercetin formulation using nanosuspension technology. *Int. J. of Ph.*, **2011**, 404, 231-237.
6. Chen, J.C.; Ho, F.M.; et al. Inhibition of iNOS gene expression by quercetin is mediated by the inhibition of IkappaB kinase, nuclear factor-kappa B and STAT1, and depends on heme oxygenase-1 induction in mouse BV-2 microglia. *Eu. J. of Ph.*, **2005**, 521(1-3):9–20.
7. Borghetti, G.S.; Lula, I.S.; et al. Quercetin/beta-cyclodextrin solid complexes prepared in aqueous solution followed by spray-drying or by physical mixture. *AAPS Ph. SciTech*, **2009,** 10(1):235–242.

8. Kellici, T. F.; Chatziathanasiadou, M. V.; et al. Mapping the interactions and bioactivity of quercetin(2-hydroxypropyl)-β-cyclodextrin complex. *Int. J. of Ph.*, **2016**, 511(1), 303–311.
9. Diamantis, D.A.; Ramesova, S; et al. Exploring the oxidation and iron binding profile of a cyclodextrin encapsulated quercetin complex unveiled a controlled complex dissociation through a chemical stimulus. *BBA – Gen. Sub.*, **2018**, 1862(9), 1913-1924.
10. Del Valle, E. M. M. Cyclodextrins and their uses: A review. *Pr. Biochem.*, **2004**, 39(9), 1033–1046.
11. Szente, L.; Szejtli, J. Highly soluble cyclodextrin derivatives: chemistry, properties, and trends in development. *Adv. D. Del. Rev.*, **1999**, 36(1), 17–28.
12. Salustio, P.J.; Pontes, P.; et al. Advanced technologies for oral controlled release: cyclodextrins for oral controlled release, *AAPS Ph. SciTech*, **2011**, 12(4), 1276-1292.
13. Sabogal-Guáqueta, A.M.; Muñoz-Manco, J.I.; et al. The flavonoid quercetin ameliorates Alzheimer's disease pathology and protects cognitive and emotional function in aged triple transgenic Alzheimer's disease model mice. *Neuroph.*, **2015**, 93, 134–145.
14. Agrawal, M.; Saraf, S.; et al. Nose-to-brain drug delivery: An update on clinical challenges and progress towards approval of anti-Alzheimer drugs. *J. of CRS*, **2018**, 281, 139–177.
15. Marttin, E.; Verhoef, J.C.; et al. Efficacy, safety and mechanism of cyclodextrins as absorption enhancers in nasal delivery of peptide and protein drugs. *J. of D. Targ.*, **1998**, 6:17–36.
16. EMA, Guideline on the Investigation of Bioequivalence, 20 January 2010, CPMP/EWP/QWP/1401/**98** Rev. 1/ Corr **
17. Figueiras, A.; Carvalho, R.A.; et al. Solid-state characterization and dissolution profiles of the inclusion complexes of omeprazole with native and chemically modified β-cyclodextrin. *Eu. J. of Ph. and Bioph.*, **2007**, 67, 531-539.
18. Salomon-Ferrer, R.; Gotz, A. W.; et al. Routine Microsecond Molecular Dynamics Simulations with AMBER on GPUs. 2. Explicit Solvent Particle Mesh Ewald. *J. Chem. Theory Comput*. **2013**, 9 (9), 3878−3888.
19. Case, D. A.; Babin, V.; et al. Amber14; University of California, San Francisco, **2014**.
20. Case, D. A.; Cheatham, T. E., et al. The Amber biomolecular simulation programs. *J. Comput. Chem.*, **2005**, 26 (16), 1668−1688.
21. Frisch, M. J.; Schlegel, H. B.; et al, Gaussian 09; Gaussian, Inc.: Wallingford, CT, **2009**.
22. Bayly, C. I.; Cieplak, P.; et al. A wellbehaved electrostatic potential based method using charge restraints for deriving atomic charges: the RESP model. *J. Phys. Chem*., **1993**, 97 (40), 10269−10280.
23. Wang, J.; Wolf, R. M.; et al. Development and testing of a general amber force field. *J. Comput. Chem.,* **2004**, 25 (9), 1157−1174.
24. Higuchi, T.; Connors, K. A. Phase solubility techniques. *Adv. in An. Chem. and Instr.*, **1965**, 4:117–212
25. EMA, *Cyclodextrins used as excipients*, 9 October 2017, EMA/CHMP/333892/**2013**.
26. Waiver of In Vivo Bioavailability and Bioequivalence Studies for Immediate-Release Solid Oral Dosage Forms Based on a Biopharmaceutics Classification System Guidance for Industry, U.S. Department of Health and Human Services Food and Drug Administration Center for Drug Evaluation and Research (CDER), December **2017**.
27. Illum, L.; Watts, P.; et al. Intranasal Delivery of Morphine, *The J. of Ph. and Exp. Ther.*, **2002**, 301, No. 1, 391-400
28. Balducci, A. G.; Ferraro, L.; et al. Antidiuretic effect of desmopressin chimera agglomerates by nasal administration in rats. *International Journal of Pharmaceutics*, 2013, 440(2), 154–160.
29. Kratz, J.M.; Teixeira, M.R.; et al. Preparation, Characterization, and In Vitro Intestinal Permeability Evaluation of Thalidomide–Hydroxypropyl-β-Cyclodextrin Complexes. *AAPS Ph SciTech*., **2012**, 13(1):118-24.

30. Talegaonkar, S.; Yakoob Khan, A.; et al. Development and Characterization of Paracetamol Complexes with Hydroxypropyl-β-Cyclodextrin. *Ir. J. of Ph. Res.*, **2007**, 6(2):95-99.
31. Soares da Silva, L.F.; do Carmo, F.A.; et al. Preparation and evaluation of lidocaine hydrochloride in cyclodextrin inclusion complexes for development of stable gel in association with chlorhexidine gluconate for urogenital use. *Int. J. of Nanome.*, **2011**, 6:1143-54.
32. Borghetti, G.S.; Lula, I.S.; et al. Quercetin/beta-cyclodextrin solid complexes prepared in aqueous solution followed by spray-drying or by physical mixture. *AAPS Ph. SciTech*. **2009**, 10(1):235-42.
33. Pralhad, T.; Rajendrakumar, K. Study of freeze-dried quercetin-cyclodextrin binary systems by DSC, FT-IR, X-ray diffraction and SEM analysis. *J. of Ph. and Biomed. An.*, **2004,** 34(2):333-339.
34. Sri, K. V., Kondaiah, A., Ratna, J. V., & Annapurna, A. Preparation and Characterization of Quercetin and Rutin Cyclodextrin Inclusion Complexes. *Drug Development and Industrial Pharmacy*, **2007**, 33(3), 245–253.
35. D'Aria, F., Serri, C., Niccoli, M., Mayol, L., Quagliariello, V., Iaffaioli, R. V., Biondi, M., Giancola, C. Host–guest inclusion complex of quercetin and hydroxypropyl-β-cyclodextrin. *Journal of Thermal Analysis and Calorimetry*, **2017**, 130(1), 451–456.
36. Sahoo, N.G.; Kakran, M.; et al. Preparation and characterization of quercetin nanocrystals. *J. of Ph. Sci.*, **2011,** 100(6):2379-90.
37. Liu, M., Dong, L., Chen, A., Zheng, Y., Sun, D., Wang, X., & Wang, B. Inclusion complexes of quercetin with three β-cyclodextrins derivatives at physiological pH: Spectroscopic study and antioxidant activity. *Spectrochimica Acta Part A: Molecular and Biomolecular Spectroscopy*, **2013**,115, 854–860
38. Oana, M.; Tintaru, A.; et al. Spectral Study and Molecular Modeling of the Inclusion Complexes of β-Cyclodextrin with Some Phenoxathin Derivatives. *The J. of Phys.l Chem. B.***, 2002**, 106, 257-263.
39. Alexandrino, G. L.; Calderini, A.; et al. Spectroscopic (fluorescence, 1D-ROESY) and theoretical studies of the thiabendazole and β-cyclodextrin inclusion complex. *J. of Incl. Phen. and Macr. Chem.*, **2013**, 75, 93-99.
40. Mercader-Ros, M. T.; Lucas-Abellán, C.; et al. Kaempferol Complexation in Cyclodextrins at Basic pH. *J. of Agr. and Food Chem.*, **2010**, 58, 4675-4680.
41. Ramakrishna, G.; Ghosh, H. N. Efficient Electron Injection from Twisted Intramolecular Charge Transfer (TICT) State of 7-Diethyl amino coumarin 3-carboxylic Acid (D-1421) Dye to TiO2 Nanoparticle. *The J. of Phys. Chem. A.*, **2002**, 106, 2545-2553.
42. Ntountaniotis, D.; Andreadelis, I.; et al. Host–Guest Interactions between Candesartan and Its Prodrug Candesartan Cilexetil in Complex with 2-Hydroxypropyl-β-cyclodextrin: On the Biological Potency for Angiotensin II Antagonism. *Mol. Pharm.*, **2019**, 16, 1255-1271.
43. Arora, P.; Sharma, S.; Garg, S. Permeability issues in nasal drug delivery. *Drug Discovery Today*, **2002**, 7(18), 967–975.
44. Illum, L. Nasal drug delivery: new developments and strategies. *Drug Discovery Today*, **2002**, (23), 1184–1189.
45. Tiozzo Fasiolo, L.; Manniello, M. D.; et al. Opportunity and challenges of nasal powders: Drug formulation and delivery. *European Journal of Pharmaceutical Sciences*, **2018**, 113, 2–17.
46. Nishijo, J.; Moriyama, S.; Shiota, S.; Kamigauchi, M.; Sugiura, M. Interaction of Heptakis (2,3,6-Tri-O-methyl)-β-cyclodextrin with Cholesterol in Aqueous Solution. *Chem. & Ph. Bulletin*, **2004**, 52(12), 1405–1410.
47. Gan, Y.; Zhang, Y.; et al. A novel preparation of methyl-β-cyclodextrin from dimethyl carbonate and β-cyclodextrin. *Carb. Res.*, **2011**, 346(3), 389–392.

48. Santos, P. S.; Souza, L. K. M.; et al. Methyl-β-cyclodextrin Inclusion Complex with β-Caryophyllene: Preparation, Characterization, and Improvement of Pharmacological Activities. *ACS Omega*, **2017**, 2(12), 9080–9094.
49. Pradines, B.; Gallard, J.-F.; et al. The unexpected increase of clotrimazole apparent solubility using randomly methylated β-cyclodextrin. *J. of Mol. Recogn.*, **2015**, 28(2), 96–102.
50. Musialik, M.; Kuzmicz, R.; et al. Acidity of Hydroxyl Groups: An Overlooked Influence on Antiradical Properties of Flavonoids. *The J. of Org. Chem.*, **2009**, 74(7), 2699–2709.
51. Herrero-Martínez, J.M.; Sanmartin, M.; et al. Determination of dissociation constants of flavonoids by capillary electrophoresis. *Electroph.*, **2005**, 26(10), 1886–1895.
52. Löbenberg, R.; Murakami, T. A Minireview: Usefulness of Transporter-Targeted Prodrugs in Enhancing Membrane Permeability. *J. of Ph. Sci.*, **2016**, 105(9), 2515–2526.
53. Dwi S.; Febrianti S.; et al. PEG 8000 increases solubility and dissolution rate of quercetin in solid dispersion system. *Marmara Pharm. J.*, **2018**, 22(2): 259-266.
54. Waldmann, S.; Almukainzi, M.; et al. Provisional biopharmaceutical classification of some common herbs used in western medicine, *Mol. Pharm. 9*, **2012**, 815–822.
55. Yu, L.X.; Amidon, G.L.; et al. Biopharmaceutics classification system: the scientific basis for biowaiver extensions, *Pharm. Res.* 19, **2002**, 921–925.
56. Macheras, P.; Karalis, V.; et al. Keeping a critical eye on the science and the regulation of oral drug absorption: a review, *J. Pharm. Sci*. 102, **2013**, 3018–3036.
57. Loftsson T.; Jarho P.; et al. Cyclodextrins in drug delivery. *Exp. opinion on d. del.*, **2005**, 2 (2), 335-351.
58. Muankaew, C. & Loftsson, T. Cyclodextrin-Based Formulations: A Non-Invasive Platform for Targeted Drug Delivery. *Basic & Clinical Pharmacology & Toxicology*, **2017**, 122(1), 46–55.
59. Ishisaka, A.; Ichikawa, S.; Sakakibara, H.; Piskula, M. K.; Nakamura, T.; Kato, Y.; Terao, J. Accumulation of orally administered quercetin in brain tissue and its antioxidative effects in rats. *Free Radical Biology and Medicine*, **2011**, 51(7), 1329–1336.

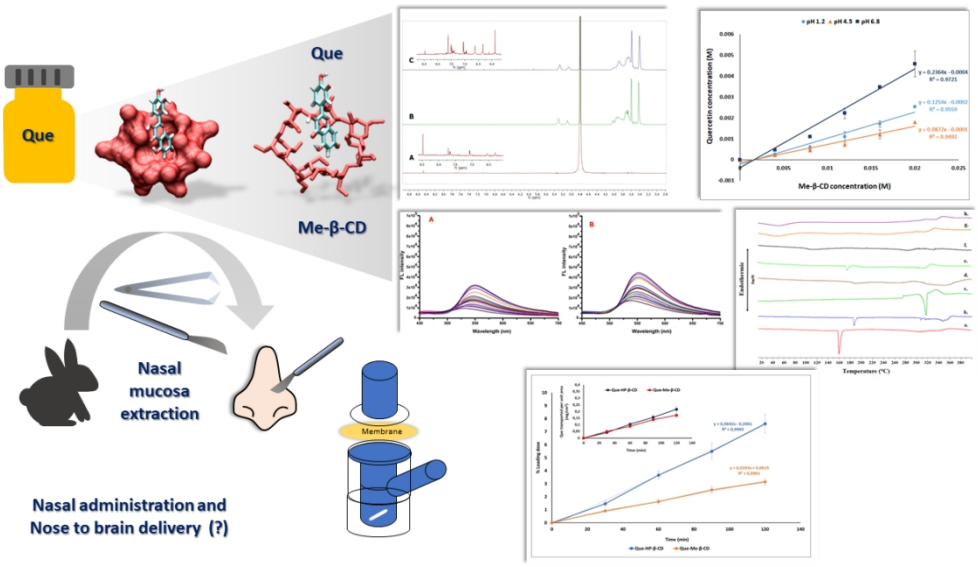

Graphical abstract

338x190mm (96 x 96 DPI)